Chapter 6

PICOSECOND LASER SPECTROSCOPY AND OPTICALLY DETECTED MAGNETIC RESONANCE ON MODEL PHOTOSYNTHETIC SYSTEMS IN BIOPOLYMERS*

G. F. W. Searle, T. J. Schaafsma, and A. van Hoek

TABLE OF CONTENTS

I. General Introduction 220
  A. Energy Transfer 220
  B. Energy Trapping 222

II. Instrumental Methods 222
  A. Picosecond Time-Correlated Photon Counting 222
  B. Optically Detected Magnetic Resonance 224

III. Pigment-Biopolymer Systems 228
  A. Model Pigment — Model Biopolymer 228
  B. Model Pigment — Natural Biopolymer 230

IV. Theory 231
  A. Fluorescence-Detected Magnetic Resonance 231
    1. Principles 231
    2. FDMR in the Presence of Energy Transfer 233
  B. Fluorescence Fading 237
  C. FDMR vs. FF 241

V. Conclusions and Perspectives 241

References 242

* Dedicated to R. Avarmaa (1941-1987).

I. GENERAL INTRODUCTION

There has been a trend the last 10 to 20 years to study biological systems of increasing size and complexity with physical techniques. A first prerequisite for such studies is naturally a well-characterized biological preparation and a second is a good understanding of the technique in order to interpret the results correctly. A combination of biological and physical expertise is not always available, however in the field of photosynthesis, which is characteristically interdisciplinary by nature, there is an exceptionally high number of such research groups.

The primary photophysical processes of plant or bacterial photosynthesis, such as excitation energy transfer and charge separation (trapping), occur on the femtosecond-nanosecond timescale.[1] These processes are of interest from a biophysical and physicochemical point of view and will be discussed by focusing on some representative models of the photosynthetic system.

Although picosecond laser spectroscopy has a relatively short history,[2] it has been applied extensively to photosynthetic systems, and more recently to their model systems, because of the ease of exciting such systems with picosecond light pulses, followed by optical detection with fluorescence or absorption.

Optically detected magnetic resonance (ODMR) can be regarded as a zero magnetic field version of the well known electron spin resonance (ESR) technique.[3]

It is not necessary to perform ODMR experiments on a picosecond timescale, as changes in triplet state populations take place in microseconds or longer.[3] Therefore, this technique cannot be used to study primary photosynthetic processes directly, but it has been shown to give information indirectly on energy transfer between pigments via molecular triplet states.[4]

This review is primarily concerned with lasers and their applications. Lasers are used in order to achieve the time resolution needed to observe photophysical processes, very similar to those occurring in photosynthesis, in real time. For example, the singlet state kinetics of chlorophylls and porphyrins are on a sub-10 ns timescale. Lasers are also used as high-intensity excitation sources in order to generate a significant population of triplets in (bio)polymers, probing the microenvironment of the excited molecule.

The central question, which we address in this review, is how the use of picosecond laser spectroscopic studies combined with the use of ODMR techniques can yield information on the transfer and storage of energy in model photosynthetic systems. These systems can be isolated from the *in vivo* apparatus biochemically and consist of chlorophyll and carotenoid molecules bound noncovalently to protein,[5] or synthesized chemically using porphyrins with various functional groups attached.[6]

The basic system is a collection of specialized pigment molecules

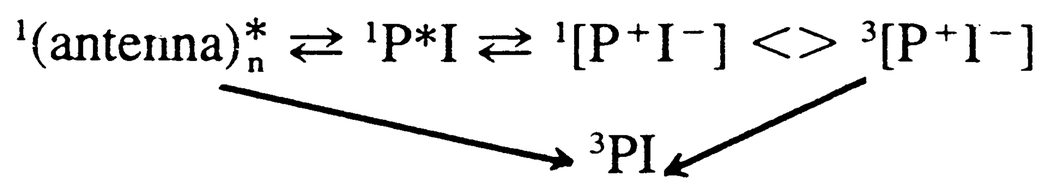

exhibiting singlet excitation energy transfer and energy trapping, for example, by charge separation and recombination in complexes of molecules; one type may act as an electron donor (P), the other as an electron acceptor (I) or intersystem crossing within the donor molecule.

A. ENERGY TRANSFER

How important is the function of the biopolymer in inducing and controlling energy transfer in the antenna pigments through pigment-biopolymer interactions? What are the physical mechanisms involved in exerting this function?

Förster-type resonance energy transfer is inversely proportional to the sixth power of the distance between a pair of molecules,[7] and it is therefore critically important for the overall efficiency of a multistep transfer that the antenna pigments are closely spaced. However, in order to prevent strong interactions between pigments, which can stimulate internal conversion, this spacing must be held at about 1 nm. Förster transfer also depends on the relative orientation of the pigments,[7] but in an unordered system containing many molecules this factor is less critical. In chlorophyll protein complexes, the protein and biopolymer play an important role in the structural organization of the pigments and determine, to a great extent, the efficiency of the Förster transfer.

The three-dimensional organization of the pigments in the biopolymer appears at first sight to be a rather random affair.[8] There is a striking absence of any regularity in the organization, and this noncrystalline structure determines the coherence time for the energy transfer.[9] This time is short, leading to energy transfer with a diffusive and incoherent character.

Another role for the biopolymer is that of inducing transfer through energy (optical spectroscopic shifts). The pigments are bound noncovalently to the biopolymer[5] and it is highly unlikely that the rather weak chlorophyll-protein interactions would lead to a significant distortion of the rigid chlorophyll ring system itself. However, interactions through ligation to the central Mg atom, and through hydrogen-bonding to the carbonyl (aldehyde and ketone) side groups, lead to small shifts in the optical spectra.[10] In this way the protein can influence Förster transfer, because this depends on the overlap integral[7] representing the degree of resonance between donor and acceptor molecules in the energy transfer chain.

The heterogeneity of the pigments introduced by binding to the biopolymer can give rise to an important characteristic of photosynthetic chlorophyll protein complexes, namely that of directionality or channeling of the excitation energy. This will occur if there is a correlation of the structural organization of chlorophylls with their energy. In most mathematical models of energy transfer,[7] this element is ignored, which seriously reduces their relevance to the study of *in vivo* systems. The overall rate for energy transfer from the site of absorption of the photon to the reaction center is considerably increased by this directionality. This would otherwise be a random diffusion of excitation in three dimensions, but it can become a pseudo-unidirectional diffusion in specialized antenna complexes.[11] It is striking that in these complexes a threefold rotational symmetry often exists, but the significance of this function has so far remained a challenging puzzle.[12]

The channeling of excitation energy can be seen as a partial localization. A more complete localization is achieved when the excitation reaches the pigments surrounding the trapping site, which is most pronounced at low temperatures. In this way the efficiency of trapping can be considerably increased as the excitation can visit the trapping site many times before it is transferred away or lost as fluorescence.[7]

Pigment heterogeneity within a single antenna complex molecule coupled to structural organization is thus a useful characteristic of *in vivo* systems, not only for its function, but also for the study of energy transfer on a picosecond timescale.

The range of interactions possible with the functional groups of the protein, both in strength and in nature, also leads to an inhomogeneous broadening of the pigment absorption and fluorescence spectral bands compared to spectra for the monomeric pigments in dilute solution.[13] This allows the overlap integral for Förster transfer for endothermic (reverse or uphill) transfer steps to take nonzero and significant values.

The possibility for reverse transfer can help in optimizing the overall efficiency of energy transfer and trapping because it allows the diffusion of excitation away from a trapping site which is not able to carry out electron transfer (a closed trap), to one which is active (an open trap). Besides these static roles for the biopolymer, there could be more dynamic roles. For example, we might question whether the vibrational levels of the biopolymer couple to

the pigment vibrational states during electronic state interconversion. This is in turn dependent upon the relative rates of energy transfer and of relaxation of the higher vibrational states of the biopolymer.[9] In a Förster transfer, which is best described by a hopping of a localized excitation, i.e., transfer between pigment molecules slow compared to vibrational relaxation, there might be little coupling, although even here the timescales for excitation energy transfer and vibrational relaxation are not very different (0.1 to 1.0 ps).

B. ENERGY TRAPPING

Let us now consider energy trapping in the basic system. How important are pigment-biopolymer interactions in optimizing the efficiency of charge separation and inhibiting the recombination of the radical ion pair? In a recent review, Miller[14] has discussed this question along with the factors which control electron transfer. In this review we shall outline briefly the principles involved, insofar as they relate to our discussion of pigment-biopolymer interactions in energy transfer.

As for energy transfer, the biopolymer has a "static" role in the control of electron transfer by determining the distance and orientation of the pigments involved and by influencing the redox potential (energy) of the pigments. Further effects can be local electrical fields (induced by point charges of the protein), on the transfer of electrons, or on the (de)stabilization of charge transfer states, also, a quantum mechanical tunneling of electrons through space involving H-bonds or through biopolymer sigma-bonds. Neither of these latter effects have a counterpart in energy transfer.

We should not expect any effects of coupling of vibrational levels of pigment electronic states to biopolymer vibrational states in the system at times >10 ps after electron transfer, as this is an expected upper limit for vibrational relaxation times in these systems. At times <10 ps this coupling can in principle be present. In the photosynthetic electron-transport chain any such effects would only be significant for electron transfer from the primary donor (P) to the primary acceptor (I), and from I to the secondary acceptor (A) because electron donation to P^+ (the oxidized primary donor) occurs on a timescale of 1 ns or longer, whilst electron transfer from A takes about 200 ps.[15] Therefore, during the primary steps the electronic states may not reach vibrational equilibrium and the effects on electron transfer may be significant.

II. INSTRUMENTAL METHODS

Many spectroscopic techniques are applied to the study of energy migration in photosynthetic model systems. This treatment is limited to picosecond time-correlated photon counting and ODMR.

A. PICOSECOND TIME-CORRELATED PHOTON COUNTING

Many molecular decay processes in photopigments can be studied by picosecond fluorescence spectroscopy.[16,17] In order to obtain reliable kinetic data it is important to be aware of several kinds of annihilation processes which may occur during excitation, e.g., singlet-singlet, triplet-triplet, and exitonic annihilation.[18-20] Time-correlated single-photon counting uses pulse energies down to the subnanojoule level. In Figure 1 a block diagram of a typical setup is shown and discussed below.

Excitation from a mode-locked continuous wave laser is used, supplying optical pulses of about 100 ps full width at half maximum (FWHM) in the case of the Ar ion laser and less than 5 ps FWHM in the case of dye lasers.[21] The energy of the pulses is too low to induce singlet-singlet annihilation with an unfocused laser beam. The repetition rate of the pulses of 76 MHz for Ar ion lasers is, however, sufficiently high to initiate triplet-triplet annihilation in, for instance, chlorophyll-protein complexes. For this reason, and also to

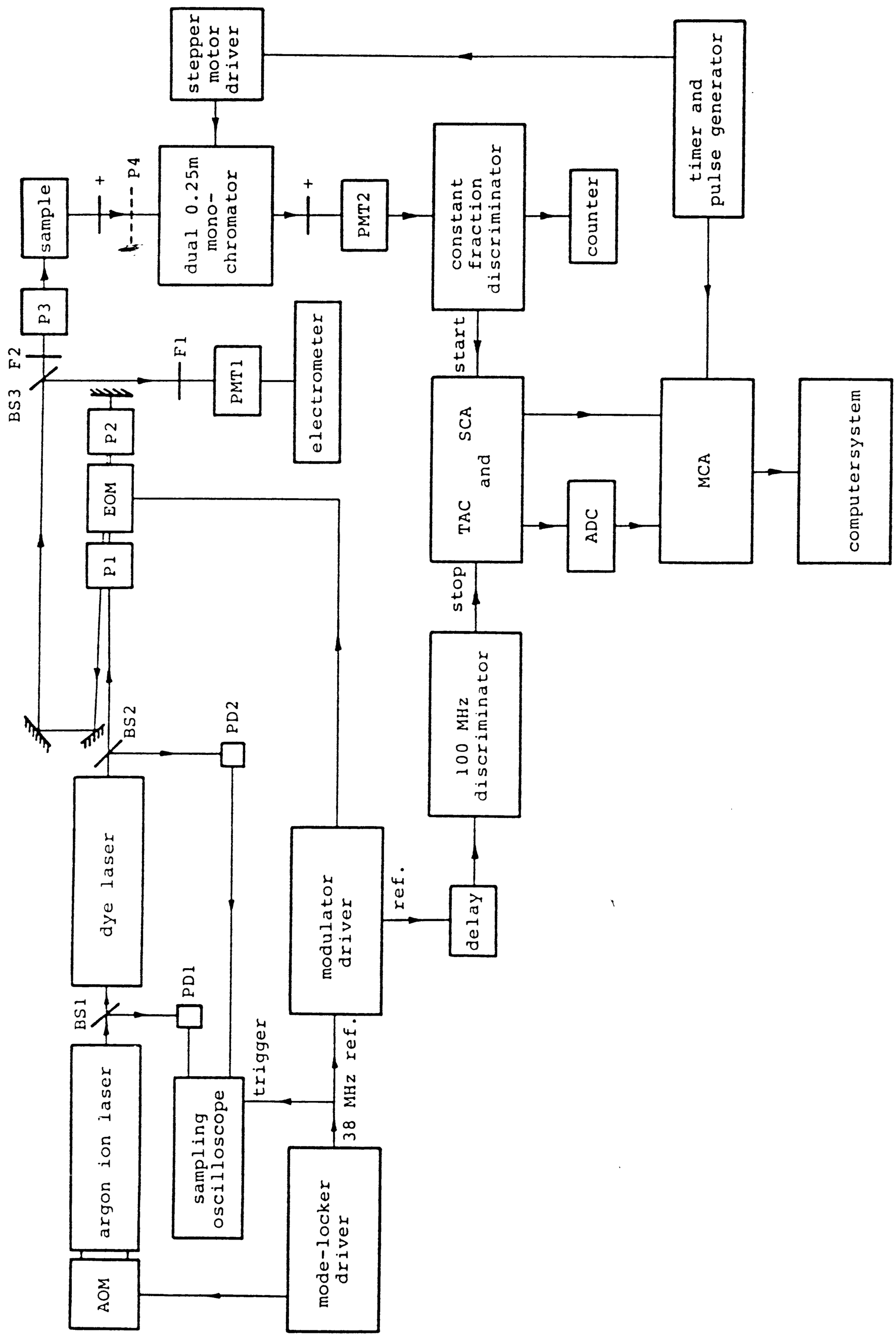

FIGURE 1. Fluorescence decay spectrometer. ADC = analog to digital converter; AOM = acoustooptic mode locker, BS1, BS2, BS3 = beamsplitters; EOM = electrooptic modulator; F1, F2 = neutral density filters; MCA = multichannel analyzer; P1, P2, P3 = optical crystal polarizers; P4 = sheet type polarizer under magic angle; PD1, PD2 = fast photodiodes; PMT1 = side window monitor photomultiplier; PMT2 = microchannel plate photomultiplier R1645UO1; TAC and SCA = time to amplitude converter with amplitude window discriminator.

increase the experimental time window, the repetition rate of optical pulses is reduced using an electrooptic modulator.[22]

The wavelength of the observed fluorescence is selected using optical filters, however, for recording time-resolved fluorescence spectra a monochromator can be used.[23] Fluorescence is detected by the photomultiplier PMT2. The start pulse for the time-to-amplitude converter is initiated with a photon pulse form PMT2 and stopped with a reference signal from the modulator driver. At the moment we use a microchannel plate-type photomultiplier (Hamamatsu R 1645U) for PMT2 resulting in an overall temporal response of about 140 ps FWHM.

With that temporal response, picosecond decay times cannot be directly determined and deconvolution of the experimental data is required. Preferably a mimic or reference deconvolution method is used,[24] resulting in a time resolution of 1 to 10 ps.[25]

B. OPTICALLY DETECTED MAGNETIC RESONANCE

ODMR is a family of techniques[26] used to study the level splittings and kinetics of molecular triplets, using optical detection of microwave-induced transitions between the triplet sublevels via optical absorption (ADMR), phosphorescence (PDMR), or fluorescence (FDMR).

The simplest form of ODMR experiment excites the sample to the first excited singlet and triplet states using a continuous light source and applies an external microwave field, of which the intensity is nominally constant but the frequency is varied. When an energy difference between two of the three triplet spin levels is in resonance with the microwave frequency, then a change in absorption, phosphorescence, or fluorescence is detected optically.

In this case the sample temperature must be low because of the fast spin-lattice relaxation at higher temperatures. The temperature of liquid helium (4.2 K) or even lower is used. By decreasing the gas pressure above the liquid helium, the temperature can be lowered to 1.2 K.

When higher temperatures are experimentally required, excitation with light and microwaves should be pulsed on a timescale short with respect to the spin lattice relaxation time, and a gated detection should be applied.[27-29] This technique requires high excitation peak powers of the microwave field.

In Figure 2 a block diagram is shown of a multipurpose ODMR setup with continuous wave laser excitation. The signal averager is used to enhance the initial low signal-to-noise (S/N) ratio by adding together the sampled signal from many (100 to 10000) sweeps of the microwave frequency.

With the trigger select switch in the left hand position (see figure) fluorescence fading experiments can be performed. The light excitation chopper blade is rotated slowly at a rate limited by the decay rate constants of the lowest triplet state (for chlorophyll *a*, for example, 10 ms open and 10 ms closed) and the signal averager is triggered via the photodiode at the light-on flank of the optical block pulse. The microwave source is not needed. Fluorescence detected during the block pulse will show a decrease in intensity compared to its initial value because the triplet population is growing in. In Figure 3 an example is given of a fluorescence fading (FF) curve, i.e., the fading of the intensity of the fluorescence on the timescale of the ingrowth of the triplet state population. The decay rate constants of the spin levels are dependent on the triplet population. So from FF curves at various exciting light intensities the rate constants are determined by extrapolating to zero relative triplet population.

With the trigger-select switch in the middle position, an FDMR experiment can be carried out to determine the molecular triplet spin level energy splittings. The light is no longer modulated by the chopper, but now the microwave field is applied and its frequency is repeatedly varied (sweeped). The signal averager is triggered each time at the beginning of the frequency sweep. A photomultiplier detects the fluorescence change when a certain

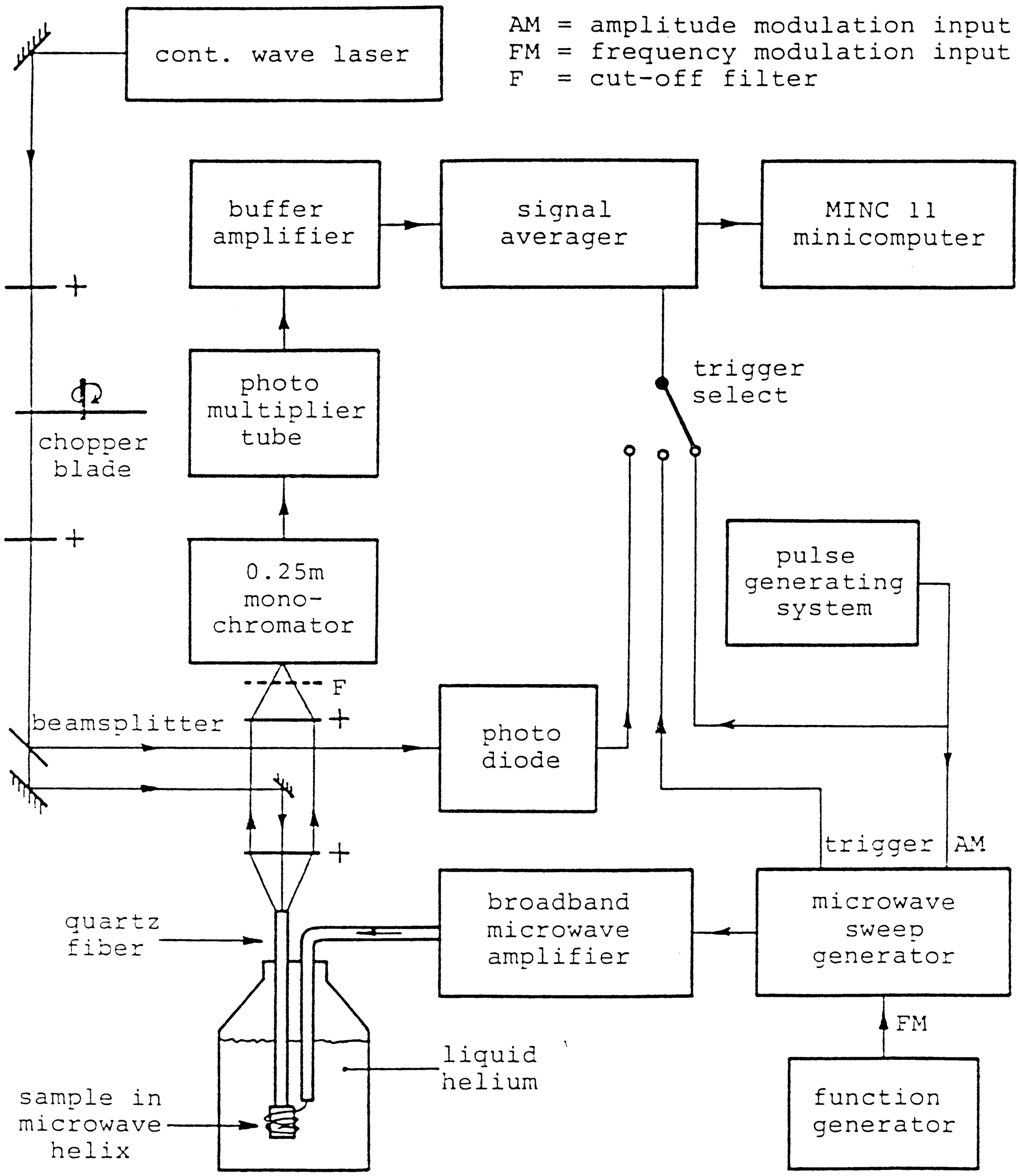

FIGURE 2. Multipurpose FDMR, FF, and MIRF apparatus.

frequency out of the sweep "fits" between two of the three triplet spin levels. These changes in the fluorescence intensity are repeatedly registered by the averager. In Figure 4 an example is presented of an FDMR spectrum.

When the trigger-select switch is in the right hand position, so-called microwave induced response of fluorescence (MIRF) experiments can be performed (Figure 5). In this case the light excitation is also unmodulated, the microwave source is fixed at the resonance frequency for coupling of two of the three triplet spin levels, and the microwave intensity is gated by the pulse-generating system. The microwave source is slightly modulated in frequency by the function generator controlling the FM input of the sweep generator to avoid too selective an excitation. Here again the very fast process of fluorescence is used as a monitor signal; in this case, to study the kinetic response of the molecular triplet sublevel populations upon short circuiting the levels by resonant external microwave radiation. This time-dependent

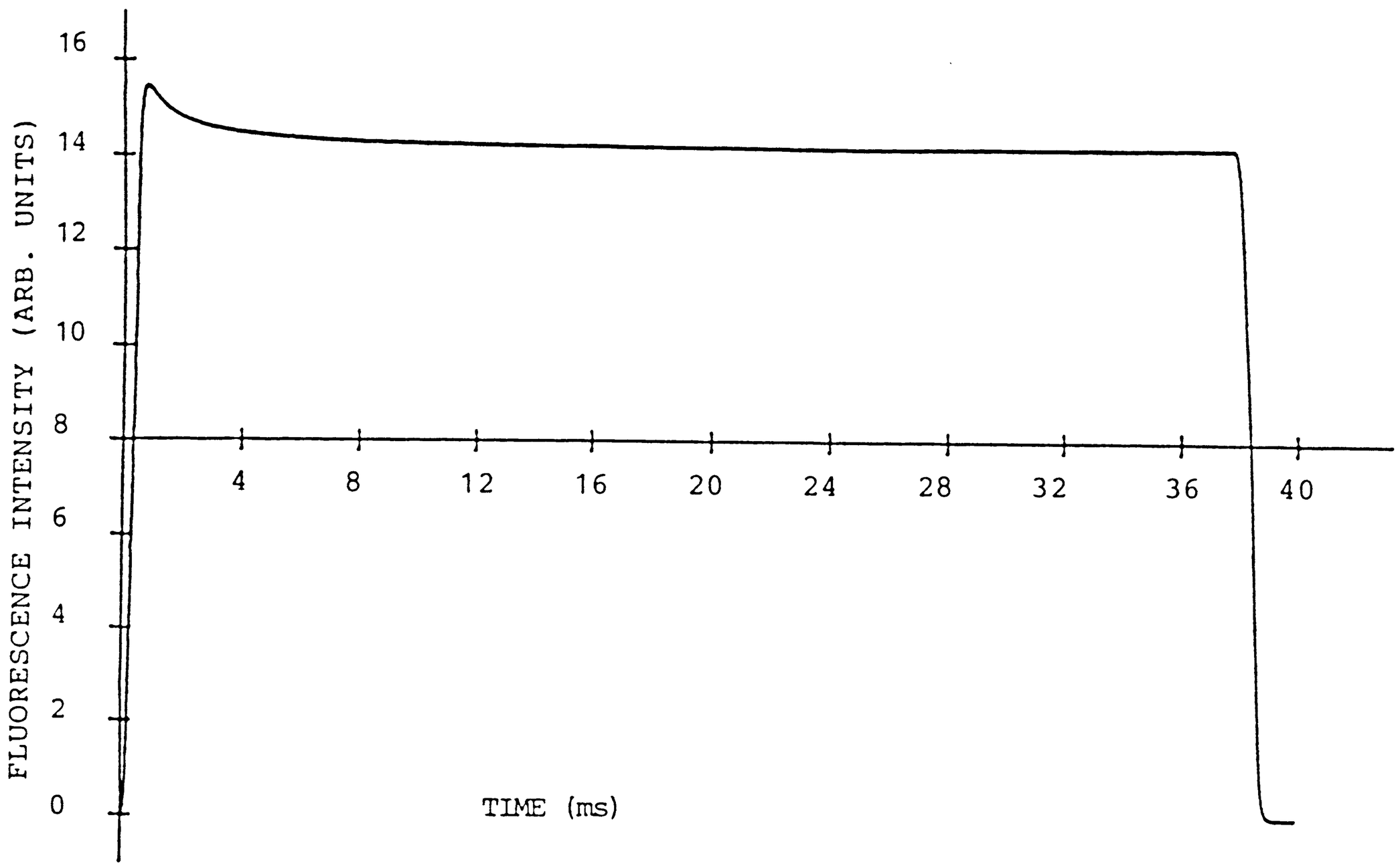

FIGURE 3. Fluorescence Fading curve of a natural chlorophyll-protein complex, isolated from plant photosystem I, at 4.2 K. Laser excitation at 458 nm, 40 mW. Detection at 718 nm, 10000 sweeps. The final percentage decrease in fluorescence was 9%. The decrease was described by a sum of three exponentials with rate constants (s^{-1}) 2133 ± 300, 522 ± 17, and 93 ± 6, and relative amplitudes 0.11, 0.71, and 0.18.

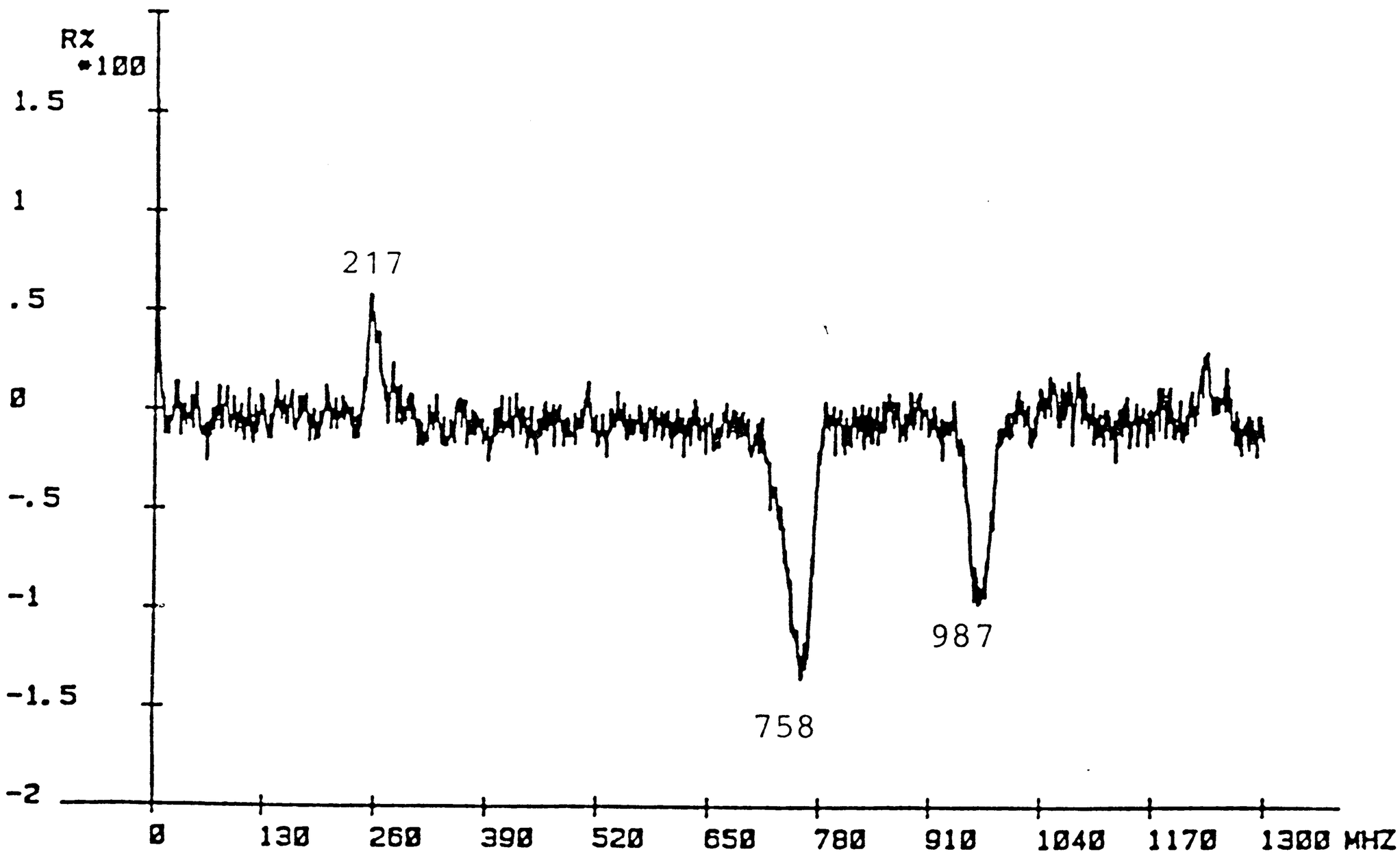

FIGURE 4. FDMR spectrum of a natural light-harvesting chlorophyll-protein complex, isolated from plants, at 4.2 K. Laser excitation at 476.5 nm, 80 mW. Detection at 683 nm, bandwidth 5 nm.

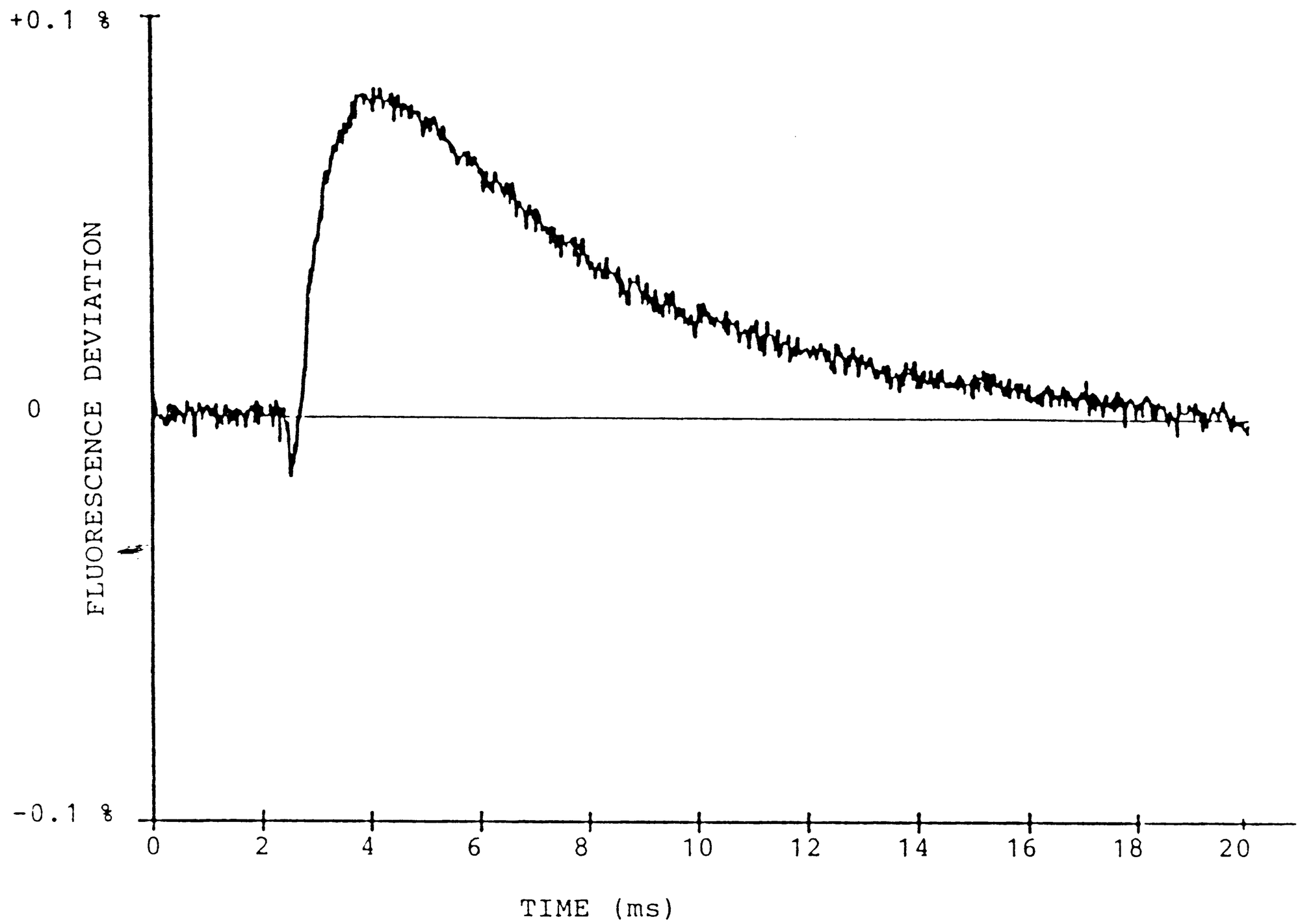

FIGURE 5. MIRF curve of a natural chlorophyll-protein complex, isolated from plant photosystem I, at 4.2 K. Microwave pulse duration 200 μs, microwave frequency in resonance with the D-E transition, and microwave power nonsaturating.

FDMR technique provides in principle the same information on triplet state decay rate constants as the FF method and both methods have their benefits and disadvantages (see Reference 30).

ODMR is experimentally, thus far, a rather simple technique. The most critical part of the setup is possibly the microwave antenna. A microwave helix is used for recording ODMR spectra because of its broad band characteristic.[31] However, a slotted tube or split ring resonator can be used when the microwave frequency is kept constant, for example, when optical spectra are recorded during microwave excitation or in the case of kinetic experiments.[32-35] The latter type of antenna is essential when a polarized H_1 field is required.[36] These tuned resonators also have the added advantage of a more efficient H_1 field generation.

The most direct way of measuring parameters of the molecular triplet state is to observe phosphorescence (or triplet-triplet absorbance). If phosphorescence cannot be detected, only absorbance and fluorescence techniques are left. In practice these are complementary techniques, either the one or the other being the most suitable for a particular system. Observing microwave-induced changes in the fluorescence intensity is an indirect detection method but has the advantage of high sensitivity resulting in a detection limit of as low as 10^{10} to 10^{11} molecules under favorable, but not exceptional, conditions.

Noise in ODMR experiments originates primarily from the light source if a tungsten lamp or stabilized laser is not used. The large dimensions of the ODMR setup can also lead to noise due to mechanical vibrations of the optical components, and this is mainly in the low (0.01 to 100 Hz) frequency range similar to the noise introduced by the use of arc lamps. In general, no improvement in the S/N ratio should be expected from modulating the excitation, coupled to phase sensitive detection, for those situations where the detected signal contains noise originating predominantly from one of the excitation sources. However,

in practice when recording FDMR, PDMR, or ADMR spectra the irradiating microwaves are indeed often amplitude modulated and the signal phase sensitively detected, giving at least the advantage of separating the microwave-induced changes from the main fluorescence signal. This also can be achieved by AC coupling of the detected signal resulting in an easier determination of the relative deviation amplitudes of the optical signals. Modulation of the microwaves and synchronous detection of the signal will improve the S/N ratio, particularly in those parts of the spectra which are between the resonance lines. The reason for this perhaps unexpected improvement is that the amplitudes of the microwave-induced deviations of the signal are small with respect to the total signal amplitude (usually only 0.1 to 1.0%). The resulting improvement in S/N ratio is dependent on the modulation frequency that can be applied, noise characteristics of the excitation sources, and relative amplitude of the microwave-induced changes.

III. PIGMENT-BIOPOLYMER SYSTEMS

There has been relatively little success in the synthesis of well-characterized models of photosynthetic systems based on biopolymers which would allow an investigation of the role of the biopolymer. There have been reports of the synthesis of poorly structured absorbates, such as chlorophyll onto serum albumin,[37] and chlorophyll onto polythene with the help of a coabsorbate,[38] but these attempts have not given experimental samples suitable for studies of the physical mechanisms of energy transfer and electron transfer. We shall therefore confine ourselves to pigment-biopolymer systems which have a known structure. From these we have selected two, which represent an improving degree of modeling of the *in vivo* photosynthetic system in two stages: (1) model pigment — model biopolymer and (2) model pigment — natural biopolymer.

A. Model Pigment — Model Biopolymer

The group of Vacek has developed a system consisting of pheophorbide *a* bound covalently, via the C-17 carboxyl group, to some of the epsilon amino groups of the lysine in a poly-tripeptide(L-lys-L-ala-L-ala), see Figure 6.

Pheophorbide is a chemically stable derivative of the natural pigment chlorophyll. The central Mg atom is replaced by protons and the long hydrophobic phytyl alcohol side chain is removed, giving a model pigment which has spectroscopic properties very similar to those of chlorophyll itself. There is, however, no possibility for ligation, so that variation of the energy through pigment-biopolymer interaction is confined to that via the ring V carbonyl group, and energy level shifts due to pigment-pigment interaction will probably dominate. The phytyl chain, which *in vivo* helps to anchor the chlorophyll molecule to protein, has its role taken over by the covalent amide bond.

The polytripeptide has been chosen to contain a hydrophilic, charged amino acid, and a hydrophobic amino acid in approximately the same ratio as found for the natural chlorophyll-binding proteins.[39] The lysine also provides the pigment anchoring site. The modeling is, of course, not perfect; the main deficiency being that *in vivo* the hydrophobic and hydrophilic regions of the protein are 20 to 30 amino acids long — the hydrophobic alpha-helical stretches are known to span the lipid membrane.[11] The polytripeptide can be brought into a folded configuration depending on the solvent so that the pheophorbide molecules can interact with each other, resulting in dimer-like low-energy trapping sites serving as models for reaction centers.

The linking of the pheophorbide to the polytripeptide introduces an unfortunate uncertainty into the model because complete substitution of the lysines is not possible and the distribution of the pheophorbides along the polypeptide is not known.

In 1981 Fidler et al.[40] reported that the pheophorbide *a* polytripeptide showed a two-

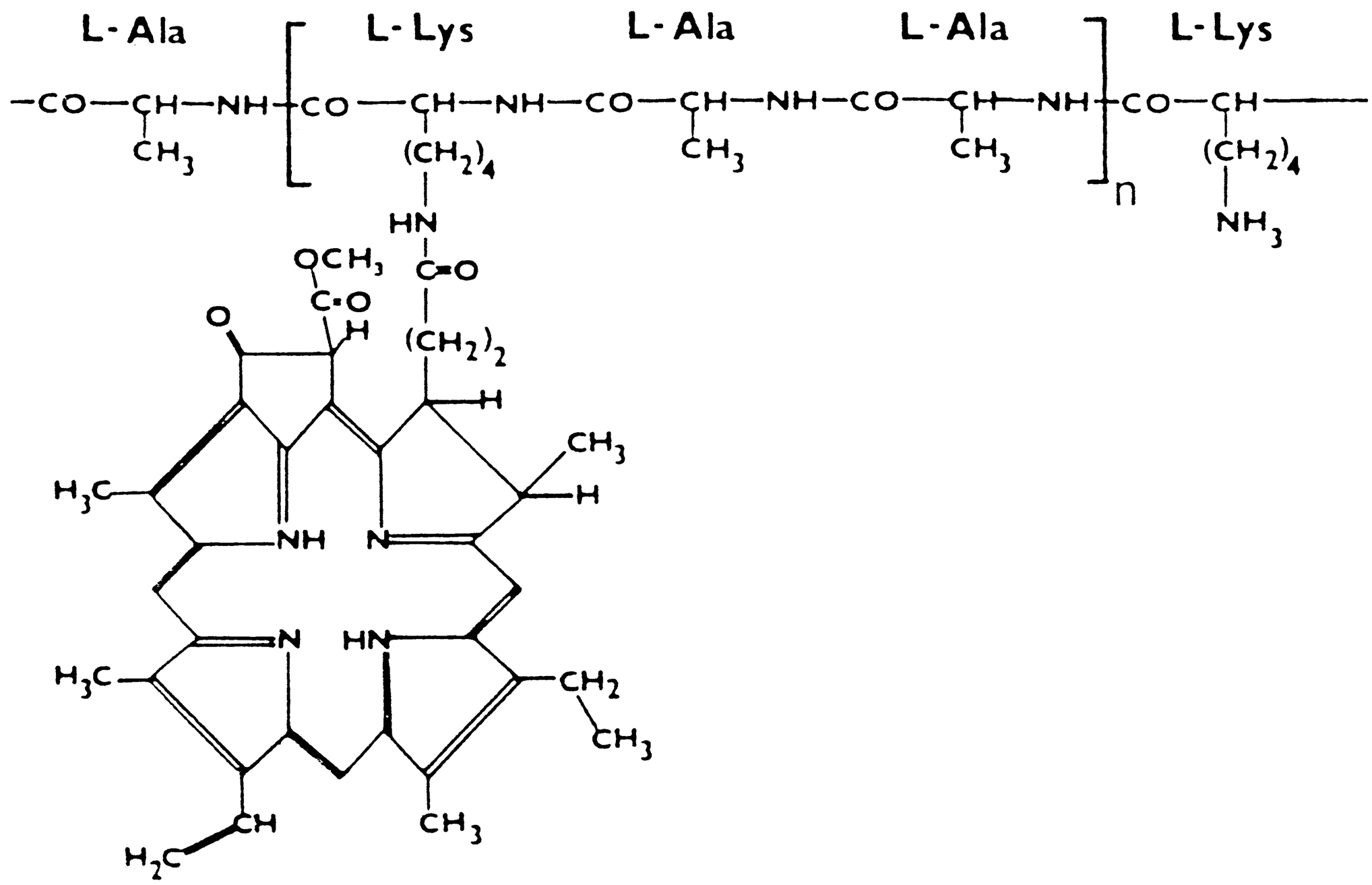

FIGURE 6. Structure of the photosynthetic model system consisting of pheophorbide *a* bound covalently to a synthetic polytripeptide; average molecular weight is 10000. Solvent: dimethylformamide. (From Hala, J., Searle, G. F. W., Schaafsma, T. J., van Hoek, A., Pancoska, P., Blaha, K., and Vacek, K., *Photochem. Photobiol.*, 44, 527, 1986. With permission.)

component fluorescence decay kinetics, using picosecond laser excitation and single photon counting detection. The longer component of 3.2 ns could be attributed to monomer pigment, while the shorter component was supposed to arise from interactions of two or more pigments which were brought into close proximity with a plane to plane distance of less than 0.2 nm.

In 1985 the Prague group reported further studies on this interesting system[41] using excitation from a dye laser, which was pumped by a nitrogen laser, in order to excite with a narrow bandwidth. They could measure fine structure in the fluorescence emission spectrum of pheophorbide a polytripeptide at 10 K in solution in dimethylformamide, and the frequencies of normal vibrations in the first excited singlet state could be compared to those for isolated (unbound) pheophorbide a. The fluorescence spectra displayed the sharp vibronic bands at different wave numbers for different dye laser excitation wavelengths, superimposed on a broad band background. It was concluded that the covalent binding of the pheophorbide-a molecule produced only slight changes in the frequencies of normal vibrations. However, significant broadening and shifts to lower energies in the site distribution function were seen, which was due to the pigment-polypeptide interaction.

In 1986 the first FDMR experiments on this system were reported jointly by the Prague group and ourselves.[42] The FDMR spectra of isolated (free) and polypeptide-bound pheophorbide a in solution in dimethylformamide were detected in the emission peak at 667 to 669 nm. There was a difference not only in microwave frequency as might be expected on interaction of the ring V carbonyl of pheophorbide a with the polypeptide — the value of the zero field splitting parameter D increased from 0.0337 in the isolated pigment to 0.0359 cm^{-1} in the bound pigment — but also in the amplitude of the transitions. The D − E transition which was negative for free pigment became positive for the bound form. The inversion of the sign was not so clear for the D + E transition, probably due to additional effects due to hydrogen bonding to the carbonyl, which are known from studies with

pheophytin[43,62] to affect the amplitude of the D + E transition. The signs of the FDMR transitions were also calculated from the relative populations and the decay rate constants of the three spin levels which were derived from FF curves. It was found that the experimental FDMR signs were opposite to those calculated from FF. This conflict could be resolved by evoking the mechanism of inversion by energy transfer, which was presented briefly in an appendix and is discussed in more detail in Section IV. It should be noted that sign inversion has also been noted in several pigment-protein complexes isolated from *in vivo* photosynthetic systems and appears to be a general phenomenon in plants and bacteria.[44]

In the same paper, further results on the picosecond fluorescence decay kinetics were reported using excitation from a synchronously pumped dye laser and single photon counting detection. If the fluorescence was monitored at different wavelengths, using a narrow bandwidth, then it was found possible to detect a heterogeneity in the emitting species. At 730 nm, a 50 ps component having 66% of the amplitude was found in the decay of bound pheophorbide *a*, but this was absent at 680 nm, and also absent at both wavelengths for the free pigment. This component was attributed to interacting pheophorbide-*a* molecules (aggregates) having an emission shifted to lower energy. These aggregates acted as traps for the excitation energy, probably through an increased rate of intersystem crossing to the triplet state.

It was proposed that the triplet state detected by FDMR in the main monomer emission band of bound pheophorbide *a* was that of the aggregate (trap) with the spectrum inverted by energy transfer.

These studies with a model pigment — model biopolymer system demonstrate the importance of the biopolymer in directing the interactions of the pigments and allowing transfer of excitation energy between them. In this model system, the folding of the polypeptide in the polar solvent dimethylformamide results in the formation of a number of pigment aggregates, acting as traps for the excitation energy.

B. MODEL PIGMENT — NATURAL BIOPOLYMER

The group of Boxer has been primarily responsible for the development of a system in which pyrochlorophyllides are bound noncovalently to myo- and hemoglobins. These globular proteins normally bind heme, an Fe-containing porphyrin molecule, with a precisely known stoichiometry; one per protein in myoglobin and four per protein in hemoglobin. The structures of the crystallized heme proteins are known from X-ray diffraction studies.[45]

The heme moieties can be removed from the protein, giving the so-called apoprotein, to quantitatively add back pyrochlorophyllide.[46] The determination of the crystal structure of the resulting complexes is still in progress, but it is a reasonable assumption that the structure is relatively unaltered as the ring systems of heme and pyrochlorophyllide are quite analogous. Therefore these model complexes have a known structure, with regard to both the pigment and the biopolymer. The pyrochlorophyllides used are stable Mg or Zn derivatives, differing from chlorophyll only in the absence of the phytyl chain and in other minor ways.

In 1979 the group of Boxer introduced the chlorophyllide *a* myoglobin system,[47] and in 1981 reported briefly on the fluorescence decay kinetics after synchrotron excitation and single photon counting detection. In addition, high field ESR measurements of a series of chlorophyllide-apomyglobin complexes in solution was reported.[48] There was apparently very little effect of the binding to the apomyoglobin on the fluorescence lifetime (single component) of the chlorophyllide derivatives tested, in most cases a slight, about 20%, lengthening was seen. The ESR-derived zero field splitting (ZFS) parameters of the bound pigments also showed little change from the values for the free pigments in organic glasses. In 1982 the same group described the absorption spectroscopic properties of pyrochlorophyllide *a*-substituted apomyoglobin in crystalline form.[45]

In 1982 the first ODMR studies of this system were carried out by the same group in cooperation with Clarke — the FDMR spectrum of the complex at 2 K was compared to that for the free pigment in an organic matrix.[49] The fluorescence emission spectrum at 2 K showed two peaks at 671 and 685 nm instead of the single broad peak at 670 to 680 nm of the free pigment, and this was interpreted as arising from two sites for the pigment. Independent evidence for two sites had previously been obtained from proton nuclear magnetic resonance (NMR) studies of these systems in solution,[48,50] and these were ascribed to different configurations of the pigment-binding site of the protein induced by the presence of the pigment. The triplet states detected by FDMR in the two resolved fluorescence bands could be distinguished by their ZFS parameters ($D = 0.0297$, $E = 0.0037\ cm^{-1}$ and $D = 0.0284$, $E = 0.0033\ cm^{-1}$, respectively) and a small difference in their decay rates. Both triplets were distinct from that of free pyrochlorophyllide *a*.

The authors came to the conclusion that the protein (biopolymer) was capable of dynamical interconversion between two conformations at room temperature, as suggested by the earlier NMR work, and that at the cryogenic temperatures of the FDMR measurements the protein complex is frozen into a statistical distribution of both conformations. The slightly different electrostatic protein environment about the pyrochlorophyllide ring results in two triplet states with different ZFS parameters. There is no difference however in the binding (ligation) of the pigment to the biopolymer in the two conformations.

This result illustrates the usefulness of ODMR in studying pigment-biopolymer interactions by using the triplet state of the incorporated pigment as an internal probe, but also introduces an element of uncertainty in the supposition that the structure of the complex is identical to that already determined for myoglobin.

In 1983 the group of Boxer extended the system to contain more than one pigment molecule per protein molecule in order to study the role of pigment-biopolymer interactions in transfer of excitation energy between the pigments.[46] They used the tetrameric apohemoglobin and complexed it with zinc pyrochlorophyllide *a*. Hemoglobin hybrids in which the heme was only partially substituted by chlorophyllide could also be synthesized. Evidence for energy transfer was obtained from steady state fluorescence anisotropy. In 1984 the picosecond fluorescence kinetics were reported[51] and energy transfer could be confirmed to occur between the two chlorophyllides in a hybrid chlorophyllide/heme apohemoglobin by following the decrease in the fluorescence anisotropy on a nanosecond timescale; the bimolecular rate constant was calculated to be 4 to $7 \times 10^8\ s_{-1}$. The fluorescence lifetime is not affected by energy transfer between chlorophyllides, and 3.73 ns was measured in fully chlorophyllide-substituted apohemoglobin compared to 3.9 ns in the chlorophyllide-apomyoglobin complex. However in chlorophyllide/heme hybrids, the lifetime was found to be shortened by exothermic energy transfer from chlorophyllide to heme (in the deoxy or cyanomet form). The authors came to the conclusion that the observed migration of excitation energy could be completely and quantitatively explained by the use of Förster's resonant excitation transfer theory so that this system should represent a suitable model to test out the effects of pigment-biopolymer interactions on energy transfer.

In a review in 1985,[52] Boxer discussed the results on these myo- and hemoglobin systems and suggested future experiments in which molecular biological techniques would be used to systematically modify amino acid residues in the vicinity of the heme pocket. He reported that very large (gram) quantities of synthetic myoglobin had already been produced using such techniques.

IV. THEORY

A. FLUORESCENCE-DETECTED MAGNETIC RESONANCE

1. Principles

Triplet state FDMR spectroscopy makes use of the fact that the threefold degeneracy of

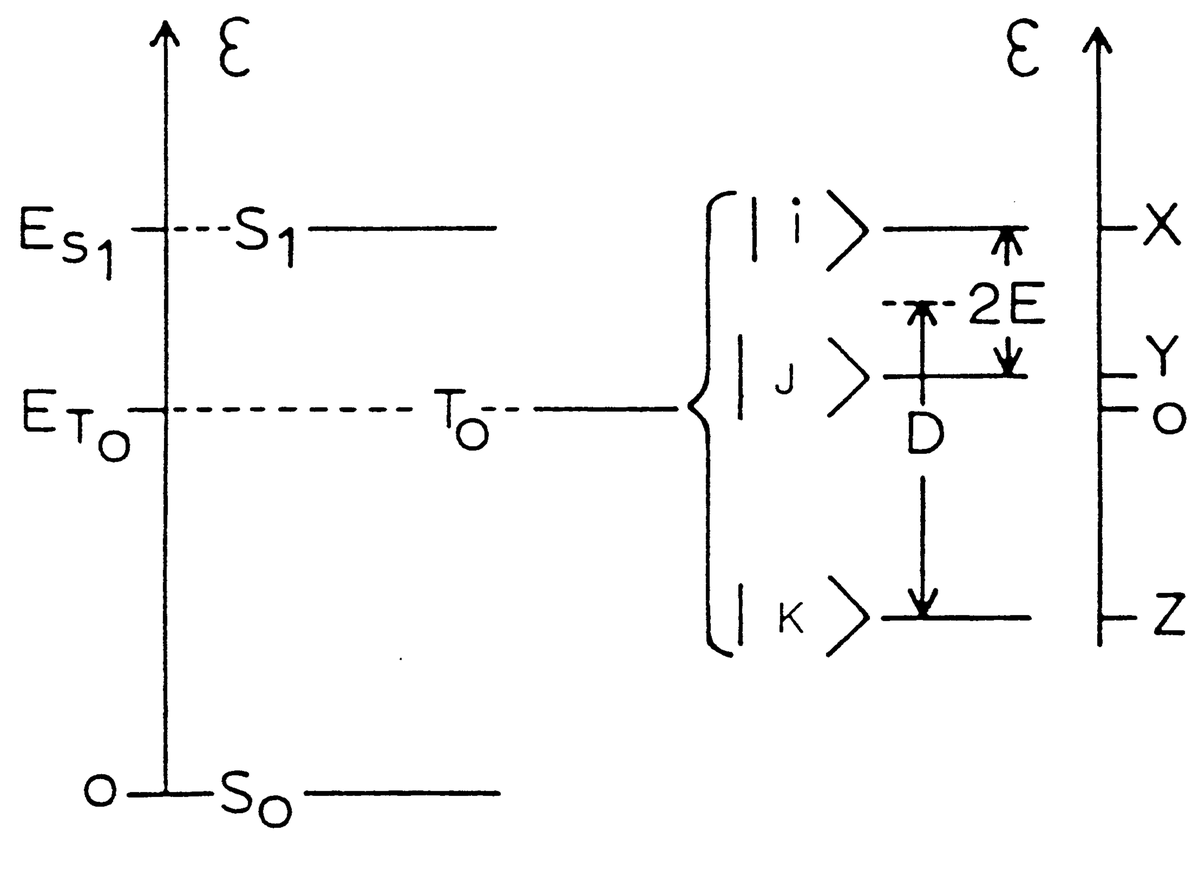

FIGURE 7. Optical pumping cycle involving the ground state (S_0), the first excited singlet state (S_1), and the lowest triplet state (T_0). The energies (ϵ) of the nondegenerate spin sublevels of T_0 (X,Y, and Z) are related to the zero field splitting parameters D and E as indicated. The zero field spin levels are labelled | i>, | j>, and | k>.

the molecular triplet state is lifted by spin-spin interaction, even in the absence of an external magnetic field. For photosynthetic pigments, the resulting zero-field splittings (ZFSs) are $\sim 10^{-2}$ cm $^{-1}$. The energies of these nondegenerate triplet spin levels are denoted X, Y, and Z and are in the order X > Y > Z, representing eigenvalues of the spin-Hamiltonian[53] of the triplet state, see Figure 7.

Thus, the distances between the spin levels (ZFSs) are given by X-Y, Y-Z, and X-Z in energy units. Conventionally, these splittings are expressed in parameters D and E, related to X, Y, and Z by[53]

$$D = -\frac{3}{2}Z \tag{1}$$

$$E = -\frac{1}{2}(X - Y) \tag{2}$$

The creation of a molecule in its lowest triplet state T_0 is usually obtained after optical excitation into an excited singlet state S_n, followed by intersystem crossing $S_n \rightarrow T_0$. Resonance transitions between the spinlevels of T_0 (X-Y, Y-Z, and X-Z) can then in principle be detected as a change in the intensity of the phosphorescence of T_0, due to microwave absorption at any of the three resonance frequencies. At low temperatures (<4 K) relaxation between T_0 spin levels can be neglected, which is a necessary condition for observing FDMR spectra.

For photosynthetic pigments, phosphorescence is too weak[54-57] to be suitable for observing zero field magnetic resonance. However, the fluorescence intensity arising from $S_1 \rightarrow S_0$ emission can be expressed as[58]

$$I_f = A\left[N - \sum_{i=1}^{3} n_i\right] \tag{3}$$

where A is an instrumental constant, N is the total number of pigment molecules, and $\sum_i n_i$ represents the number of molecules in the spin levels of the lowest triplet state (T_0). It is assumed that the number of molecules in excited singlet states can be neglected w.r.t. that in S_0 and T_0 under steady-state illumination of the sample.

Absorption of microwaves between two spin levels $|i\rangle$ and $|j\rangle$ gives rise to a change of fluorescence ΔI_f given by[59-62]

$$\Delta I_f = A(k_i - k_j)(k_i + k_j)^{-1}(n_i^0 - n_j^0) \tag{4}$$

where $i \neq j = 1,2,3$ and $n_{i,j}^0$ represents the steady-state population of the T_0 spin levels $|i\rangle$ or $|j\rangle$ under continuous illumination and in the absence of microwaves; $k_{i,j}$ are the decay rate constants of these spin levels. This equation shows that resonances may be observed only when $n_i^0 \neq n_j^0$ and $k_i \neq k_j$.

Using microwave pulses saturating the $|i\rangle \leftrightarrow |j\rangle$ transition, the resulting time dependence of the fluorescence contains the triplet state kinetics. Following the onset of the microwave pulse, the change of fluorescence is given by[61]

$$\Delta I_f(t) = A(k_i - k_j)(k_i + k_j)^{-1}(n_i^0 - n_j^0)\left\{\exp\left[-\frac{1}{2}(k_i + k_j)t\right] - 1\right\} \tag{5}$$

whereas

$$\Delta I_f(t) = Ak_ik_j(k_i + k_j)^{-1}(n_i^0 - n_j^0)\{k_i^{-1}\exp(-k_it) - k_j^{-1}\exp(-k_jt)\} \tag{6}$$

after switching off the microwaves.

The time dependence of the fluorescence $\Delta I_f(t)$ can be analyzed, yielding the decay rate constants k_λ and steady-state populations n_λ^0 of the triplet state, provided that the duration of the microwave pulse is much shorter than the smallest value of the lifetime of spin level λ. For a distribution of spin level decay rate constants, as may occur for a pigment in different microenvironments of a (bio)polymer, there is no easy check whether this condition is fulfilled. For a number of sites, the microwave pulsewidth may in fact be long, compared to the lifetime of one or more of the triplet spin levels. Under these conditions, the microwave pulse acts as a microwave step. Then, in order to obtain reliable kinetic data, the microwave step must be fully saturating the zero field transition between a pair of triplet spin levels.[63]

2. FDMR in the Presence of Energy Transfer

Figure 8 represents the lowest energy levels S_0, S_1, and T_0 of a molecule (t), acting as a trap for singlet excitation energy, transferred to this trap from a collection of excited molecules, denoted as antenna (a). Energies of the S_1^a and S_1^t, or T_0^a and T_0^t states as well as intermolecular distances are assumed to allow energy transfer to occur. We assume both the number of antenna molecules, $N_a >> N_t$, the number of trap molecules, both per unit of volume. Therefore, only the antenna is considered to be excited. Neglecting diffusional processes, singlet energy transfer can be described by the bimolecular reaction:

$$S_1^a + S_0^t \underset{k_1}{\overset{k_2}{\rightleftarrows}} S_0^a + S_1^t \tag{7}$$

followed by

$$S_1^a \underset{k_{ST}^a}{\longrightarrow} T_0^a \tag{8}$$

and/or

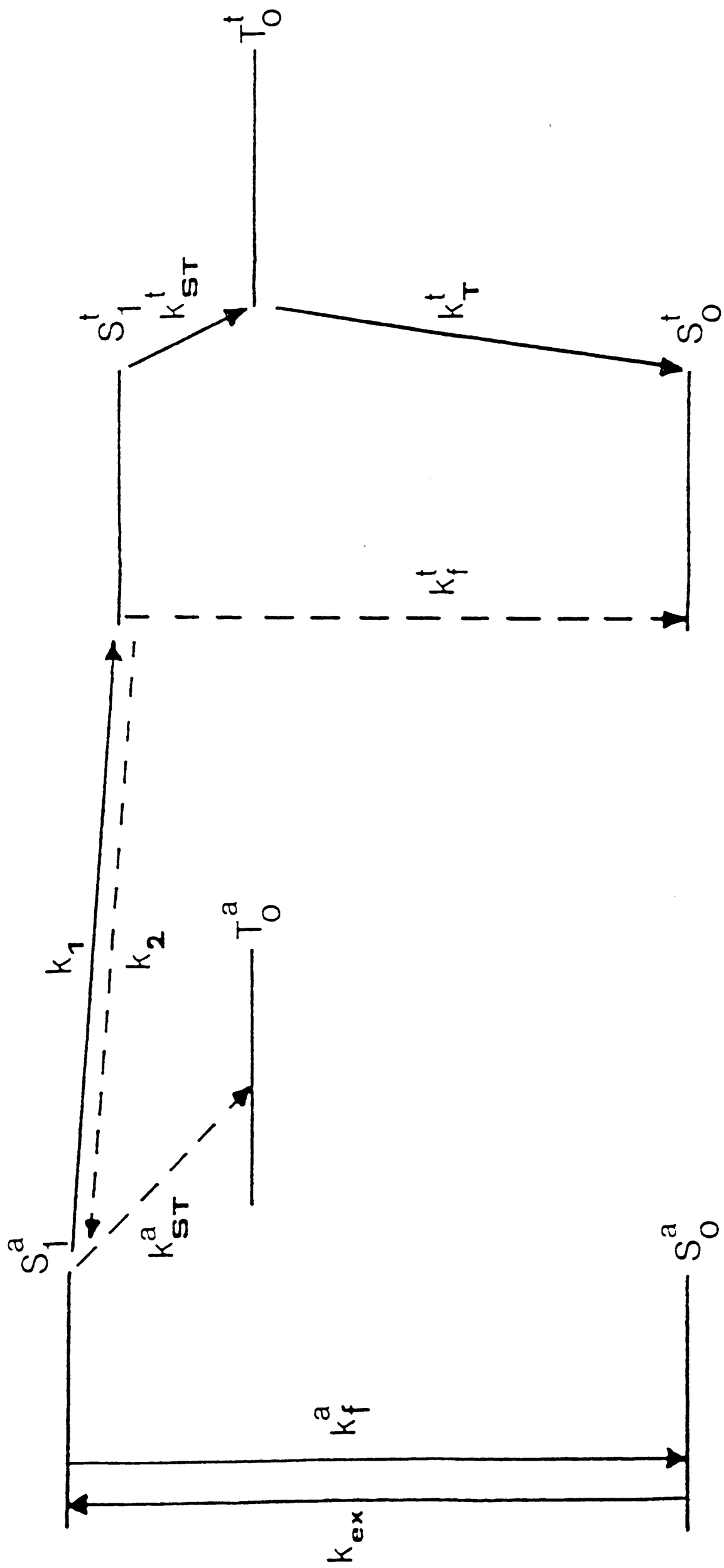

FIGURE 8. Kinetic scheme for singlet energy transfer from (a) antenna to (t) trap, and for intersystem crossing $S_1^t \rightarrow T_0^t$, in covalently bound pheophorbide-*a*. Kinetic constants are defined in the text.

$$S_1^t \xrightarrow[k_{ST}^t]{} T_0^t \tag{9}$$

Furthermore

$$S_1^a + S_0^a + T_0^a \equiv N_a \tag{10}$$

and

$$S_1^t + S_0^t + T_0^t \equiv N_t \tag{11}$$

where S_0, S_1, and T_0 denote the number of antenna and trap molecules per unit volume in the various electronic states.

Combining the rate equations

$$\dot{S}_1^a = S_0^a(k_{ex} + k_2S_1^t) - S_1^a(k_f^a + k_{ST}^a + k_1S_0^t) \tag{12}$$

$$\dot{S}_1^t = k_1S_0^tS_1^a - S_1^t(k_f^t + k_{ST}^t + k_2S_0^a) \tag{13}$$

$$\dot{S}_0^a = k_1S_1^aS_0^t - k_2S_0^aS_1^t + k_T^aT_0^a \tag{14}$$

$$\dot{S}_0^t = -k_1S_1^aS_0^t + k_2S_0^aS_1^t + k_T^tT_0^t \tag{15}$$

with Equations 10 and 11 and neglecting S_1^a and S_1^t w.r.t. S_0^a and S_0^t, respectively, yields relations between S_1^a and S_1^t on one hand and T_0^a and T_0^t on the other hand, under steady-state conditions, i.e., under continuous illumination.

Saturating any of the three transitions between the spin levels $|i>$, $|j>$ and $|k>$ of T_0^a or T_0^t results in a change of the total population of the triplet levels ΔT_0^a or ΔT_0^t.

By straightforward but tedious algebra, one finds for the resulting change of the steady-state fluorescence of antenna and trap, respectively:[42]

$$\Delta I_f^{a,t} = k_f^a\Delta S_1^a = k_{ex}\phi_f^a\phi_E(1 - \phi_E)(1 - \phi_{E'})(1 - \phi_E\phi_{E'})^{-2}\left(\frac{N_a}{N_t}\right) \cdot \Delta T_0^t \tag{16}$$

$$\Delta I_f^{a,a} = k_f^a\Delta S_1^a = -k_{ex}\phi_f^a(1 - \phi_E)(1 - \phi_E\phi_{E'}^2)(1 - \phi_E\phi_{E'})^{-2}\Delta T_0^a \tag{17}$$

$$\Delta I_f^{t,a} = k_f^t\Delta S_1^t = -k_{ex}\phi_f^t\phi_E(1 - \phi_{E'})^2(1 - \phi_E\phi_{E'})^{-2}\Delta T_0^a \tag{18}$$

$$\Delta I_f^{t,t} = k_f^t\Delta S_1^t = -k_{ex}\phi_f^t\phi_E(1 - \phi_E)(1 - \phi_{E'})(1 - \phi_E\phi_{E'})^{-2}\left(\frac{N_a}{N_t}\right)\Delta T_0^t \tag{19}$$

with

$$\phi_f^a \equiv \frac{k_f^a}{k_f^a + k_{ST}^a} \tag{20}$$

$$\phi_f^t \equiv \frac{k_f^t}{k_f^t + k_{ST}^t} \tag{21}$$

$$\phi_E \equiv \frac{k_1 N_t}{k_f^a + k_{ST}^a + k_1 N_t} \tag{22}$$

$$\phi_{E'} \equiv \frac{k_2 N_a}{k_f^t + k_{ST}^t + k_2 N_a} \tag{23}$$

ϕ_f^a and ϕ_f^t represent the fluorescence yields of antenna and trap molecules, respectively, in the absence of energy transfer, whereas ϕ_E and $\phi_{E'}$ denote the yields for forward and backward singlet energy transfer.

The equations (16 to 19) represent the four possible combinations of detecting a change in fluorescence intensity of either antenna or trap, resulting from a change in triplet population in either of these.

Several conclusions can be drawn from Equations 16 to 19:

1. If $\phi_{E'} \cong 1$ (complete back transfer), no triplets can be formed in the trap molecules (Equations 16, 18, and 19) and only $\Delta I_f^{a,a}/\Delta T_0^a \neq 0$, so that only antenna triplets can be detected when monitoring the antenna fluorescence. On the other hand, if $\phi_E \cong 1$, only $\Delta_f^{t,a}/\Delta_0^a \neq 0$. However, no antenna triplets are formed (Equation 23) and there is no FDMR transition observed at all.
2. In the absence of energy transfer, i.e., if $\phi_E = 0$, only $\Delta I_f^a/\Delta T_0^a \neq 0$, implying that FDMR spectra only contain transitions due to triplets in the antenna. These transitions have opposite sign w.r.t. those due to triplets of trap molecules observed via antenna fluorescence, i.e., in the presence of singlet energy transfer.
3. For intermediate values of ϕ_E and neglecting back transfer ($\phi_{E'} = 0$) triplets of antenna — as well as trapmolecules — can in principle be detected by monitoring the fluorescence of both types of molecules. Then the Equations 16 to 19 simplify to:

$$\Delta I_f^{a,t} = k_{ex}\phi_f^a\phi_E(1 - \phi_E)\left(\frac{N_a}{N_t}\right)\Delta T_0^t \tag{24}$$

$$\Delta I_f^{a,a} = -k_{ex}\phi_f^a(1 - \phi_E)\Delta T_0^a \tag{25}$$

$$\Delta I_f^{t,a} = -k_{ex}\phi_f^t\phi_E\Delta T_0^a \tag{26}$$

$$\Delta I_f^{t,t} = -k_{ex}\phi_f^t\phi_E(1 - \phi_E)\left(\frac{N_a}{N_t}\right)\Delta T_0^t \tag{27}$$

4. Equations 24 and 27 contain the ratio N_a/N_t, which may be a large number, thus amplifying the fluorescence change, resulting from a change in triplet population. In fact, both expressions have a different sign and differ by the ratio ϕ_f^a/ϕ_f^t. Since the trap is at lower energy than the antenna, radiationless processes are expected to be more efficient for the trap, resulting in $\phi_f^t < \phi_f^a$. Often, there are secondary processes in the trap, e.g., charge-separation, if the trap is a photochemically active photosynthetic reaction center, which results in $\phi_f^t << \phi_f^a$ and no trap fluorescence is observable.

Equations 16 to 19 and 23 to 27 can be applied to both model and *in vivo* systems.

For photosynthetic pigments embedded in a protein (constituting a photochemically active reaction center surrounded by antenna) $\phi_{E'} = 0$ and $\phi_f^t \approx 0$, and triplets formed in the reaction center (see Reference 3) can only be observed via antenna-fluorescence (Equation 16). If part of the antenna-protein is denatured during preparation, the embedded antenna-pigments cannot transfer their singlet energy to the trap and may form antenna triplets. Usually, denaturing the protein causes a blue-shift of the fluorescence emission of the embedded pigments. This blue-shifted fluorescence then can be used to obtain the FDMR spectrum of the antenna triplets (Equation 25), whereas the native fluorescence emission gives rise to the FDMR spectrum of the triplet state of the reaction center. Both spectra are expected to be very similar, but of opposite sign,[42,44,64] as is evident by comparing Equations 24 and 25.

For model systems, modification of the (bio)polymer structure, leading to unfolding of the polymer-chain, is predicted to result in $\phi_E = 0$, thus eliminating inverted FDMR transitions due to trap molecules in the triplet state.

The triplet state of the pigment can therefore be used as a probe, reflecting the ordering of the (bio)polymer, provided the distribution of intermolecular distances between the pigment molecules allows singlet energy transfer to occur. The spatial resolution is expected to be in the range of tens of nanometers, the distance over which Förster singlet energy transfer can occur.

The results using Equations 24 to 27 can also be rationalized on a more simple basis. Inspecting Figure 8 again, a positive change ΔI_f^a, resulting from a positive change ΔT_0^t can be understood as follows: increasing T_0^t leads to a decrease of S_0^t and less deactivation of S_1^a via singlet energy transfer, and fluorescence from S_1^a therefore increases. On the other hand, for isolated pigment molecules, i.e., in the absence of energy transfer, a positive change ΔT_0^a results in a decrease of S_0^a, and thus in a decrease of the steady-state fluorescence from S_1^a.

By a similar reasoning it is straightforward to see that for triplet-triplet ($T_0^a \rightarrow T_0^t$) energy transfer, no sign inversion of the FDMR transitions of the triplet state of trap molecules is observed. For T-T energy transfer, a positive change ΔT_0^t again results in a decrease of S_0^t and an increase of T_0^a under steady-state excitation of the antenna part, and this leads to a decrease of S_1^a. Similarly, $\Delta I_f^a/\Delta T_0^a$, $\Delta I_f^t/\Delta T_0^a$, and $\Delta I_f^t/\Delta T_0^t$ are all <0.

B. FLUORESCENCE FADING

Contrary to what its name suggests, FF involves only fully reversible photophysical processes and does not include irreversible photochemical changes of the investigated compound.[60,65,66] The method employs the response of the fluorescence to an optical excitation step from the singlet-ground state S_0 to an excited singlet state S_n. Assuming an instantaneous response of the S_1 population to this excitation step, the subsequent change of the fluorescence intensity $I_f(t)$ monitors the time-dependent change of the S_1 population due to transfer of molecules to the lowest triplet state T_0 by intersystem crossing. $I_f(t)$ contains the kinetics of the T_0 state. For an isolated pigment molecule, embedded in a (bio)polymer we consider the states S_0, S_1, and T_0, forming an optical pumping cycle.

The rate equations for the S_0 and S_1 states are

$$\dot{S}_0 = k_{ex}S_0 + k_fS_1 + k_TT_0 \tag{28}$$

$$\dot{S}_1 = k_{ex}S_0 - (k_f + k_{ISC})S_1 \tag{29}$$

The kinetic constants are defined in Figure 9A. The total number of molecules (N) per unit of volume is given by

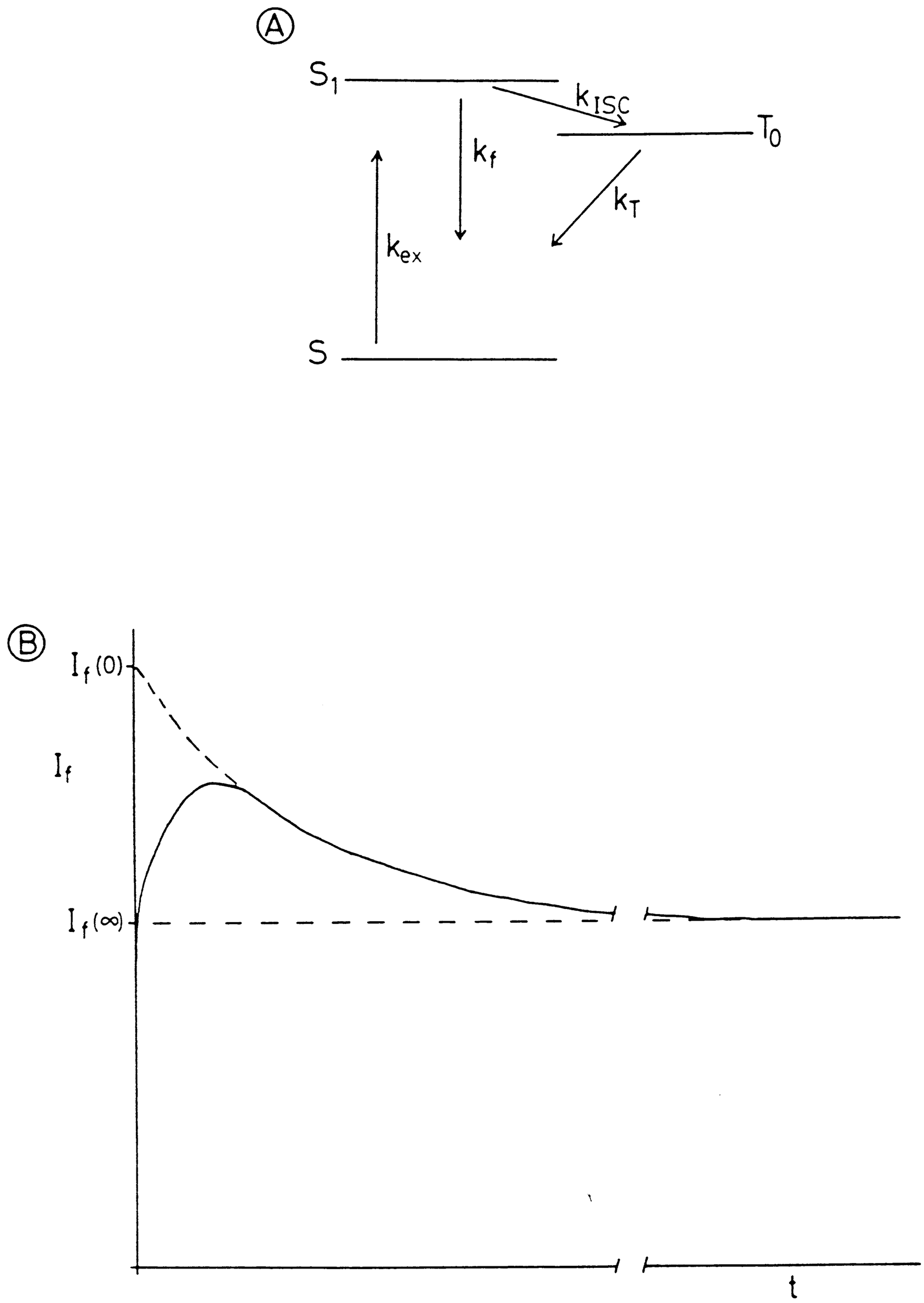

FIGURE 9. (A) Kinetic scheme underlying an FF experiment. The rate constants are optical excitation $S_0 \rightarrow S_1$, k_{ex}; radiative decay $S_1 \rightarrow S_0$, k_f; intersystem crossing, k_{isc}; and decay (radiative + nonradiative) of T_0, k_T. (B) Definition of $I_f(0)$, $I_f(\infty)$, and $I_f(t)$ following an optical excitation step starting at the origin (t = 0).

$$N = S_0 + S_1 + T_0 \tag{30}$$

where S_0, T_1, and T_0 denote the number of molecules in the corresponding states.

The response of the fluorescence intensity to an excitation step can be obtained by solving the rate equations (28 and 29) and using the relation (30). This results in:

$$S_1(t) - S_1(\infty) = A\exp(r_1 t) + B\exp(r_2 t) \tag{31}$$

$$r_1 = -k - k_{ex}(1 - \phi_T) \tag{32}$$

$$r_2 = k_T - k_{ex}\phi_T \tag{33}$$

$$k = k_f + k_{ISC} \tag{34}$$

$$A = (r_1 - r_2)^{-1}[k_{ex}N + r_2S_1(\infty)] \tag{35}$$

$$B = -(r_1 - r_2)^{-1}[k_{ex}N + r_1S_1(\infty)] \tag{36}$$

The roots r_1 and r_2 represent approximate solutions, retaining only terms linear in the excitation rate k_{ex}, which is assumed to be small w.r.t. $k_f + k_{ISC}$; the triplet quantum yield $\phi_T = k_{ISC}/k$. The constants A and B are obtained from the boundary condition $S_1(0) = 0$ and $\dot{S}_1(0) = k_{ex}N$. Noting that in general $r_1 >> r_2$, Equation 29 can be transformed into:

$$S_1(t) = k_{ex}Nk^{-1}[1 - \exp(r_1t) - k_{ex}k_{ISC}k^{-1}k_T^{-1}\{1 - \exp(r_2t)\}] \tag{37}$$

In steady state it follows that:

$$T_0(\infty) = S_1(\infty)k_{ISC}k_T^{-1} \tag{38}$$

$$S_1(\infty) = k_{ex}Nk^{-1} \tag{39}$$

Converting $S_1(t)$ into $I_f(t)$ — the fluorescence intensity — by $I_f = k_fS_1 = \phi_fkS_1$, where ϕ_f is the fluorescence quantum yield, Equation 37 takes the form:

$$I_f(t) = k_eN\phi_f\left[1 - \exp(r_1t) - \frac{T_0(\infty)}{N}\{1 - \exp(r_2t)\}\right] \tag{40}$$

Equation 38 reveals the presence of two different processes: (1) a rapid rise of the fluorescence to a steady state level, due to populating of S_1 immediately after the onset of excitation, i.e., in a time interval $k^{-1} < t < k_T^{-1}$ and (2) a much slower decrease of $I_f(t)$ due to populating T_0 — referred to as FF. Assuming $k >> k_T$, we choose to ignore the first process for $I_f(t)$, for instance, i.e., we choose the time interval such that it only refers to process (2), implying that effectively $t = 0$ somewhere in the interval $k^{-1} << t < k_T^{-1}$. Then, Equation 40 can be written as

$$I_f(t) = I_f(0)\left[1 - \frac{T_0(\infty)}{N}\{1 - \exp(r_2t)\}\right] \tag{41}$$

where $I_f(0)$ is the fluorescence intensity, found by extrapolating the fluorescence fading curve to $t = 0$. From Equation 41 we obtain:

$$I_f(t) - I_f(\infty) = [I_f(0) - I_f(\infty)]\exp(r_2t) \tag{42}$$

$$\frac{I_f(0) - I_f(\infty)}{I_f(0)} = T_0(\infty)/N \tag{43}$$

These results are a simplified version of those obtained by Avarmaa.[66] The shape of $I_f(t)$, expressed by Equation 42 is presented in Figure 9B.

By combining Equations 33 and 43, it can be easily seen that r_2 in Equation 33 can also be written as

$$r_2 = -k_T\left[1 - \frac{T_0(\infty)}{N}\right] \tag{44}$$

at low excitation rates. Thus, the true molecular triplet decay rate k_T can be simply obtained from the experimental FF curve by subtracting a fraction $\frac{T_0(\infty)}{N}$ from the measured value of r_2. This fraction also represents the experimental fractional decrease of the fluorescence intensity from its initial to its steady state value, due to transfer of molecules to T_0 during excitation.

A similar treatment as given above applies to the case where the presence of three spin levels $|i>$, $|j>$, and $|k>$ in T_0 is taken into account. Now the $I_f(t)$ curve contains the roots $k_\lambda + \phi_T^\lambda k_e$ ($\lambda = i,j,k$), analogously to Equation 42, where k_λ is the decay rate constant of spin level $|\lambda>$. Then a three-exponential analysis of $I_f(t)$, e.g., using Provencher's methods,[67] yields the three decay rate constants of the T_0 spin levels after proper extrapolation to zero optical excitation rate. The amplitudes of these three roots in $I_f(t)$ are a direct measure of the corresponding steady-state populations $n_\lambda(\infty)$.

By combining $n_\lambda(\infty)$ and k_λ for $\lambda = i,j,k$, the relative populating rates $p\lambda$ of the corresponding spin levels can be determined from $p_\lambda = n_\lambda \cdot k_\lambda$. Thus, the populating and decay kinetics of T_0 can be fully resolved without making use of transitions between the T_0 sublevels, as in FDMR. There may occur complications, however, e.g., when one of the spin levels carries no steady-state population, e.g., due to a rigid selection rule, resulting in zero populating rate. Then, of course, the decay rate constant of this level cannot be determined and one finds two, instead of three, decay components. This situation cannot be distinguished from that with two accidentally equal decay rate constants. The FF method has been employed to study the solvation of several photosynthetic pigments in noncrystalline solid solutions at low temperatures (e.g., see References 10, 65, 66, and 68).

The FF method can also be applied to systems containing both isolated pigments and traps for excitation energy, such as described by Hala et al.[42] Energy transfer may occur between the isolated pigments acting as an antenna for optical excitation and the traps. At low to moderate pigment concentration, singlet energy transfer is more likely to occur than triplet energy transfer and we will limit the following treatment to the former type of energy transfer.

Singlet energy transfer is described by the bimolecular forward and backward reactions as treated in Section IV.A2. It is assumed that the singlet energy transfer from antenna to trap is sufficiently efficient to neglect the formation of antenna triplets, i.e., no T_0^a states are considered. Neglecting back transfer ($k_2S_1^t << k_{ex}$), equating S_0^a to N_a (no formation of antenna triplets), Equation 12 simplifies to

$$\dot{S}_1^a = k_{ex}N_a - (k_f^a + k_{ST}^a)S_1^a - k_1S_0^tS_1^a \tag{45}$$

Noting that

$$\dot{S}_0^t = -k_1S_1^aS_0^t + k_2S_0^aS_1^t + k_T^aT_0^a \approx k_1S_1^aS_0^t \tag{46}$$

Equation 45 can be rewritten as

$$\dot{S}_1^a = k_{ex}N_a - (k_f^a + k_{ST}^a)S_1^a + \dot{S}_0^t \tag{47}$$

The last term in Equation 47 is dominant at $t >> (k_f^a + k_{ST}^a + k_{ex})^{-1}$, so that

$$\dot{S}_1^a = \dot{S}_0^t \tag{48}$$

Noting that $T_0^t(0) = 0$

$$S_1(t) - S_1(0) = -T_0^t(t) = T_0^t(\infty)(e^{-k_T^t t} - 1) \tag{49}$$

and the fluorescence fading $I_f(t)$ is given by

$$I_f^a(t) - I_f^a(0) = k_f^a[S_1^a(t) - S_1^a(0)] = k_f^a T_0^t(\infty)[e^{-k_T^t t} - 1] \tag{50}$$

As for an isolated molecule, the antenna fluorescence is a continuously decreasing function of time. A log plot of $\frac{I_f^a(t) - I_f^a(\infty)}{I_f^a(0) - I_f^a(\infty)}$ vs. t yields k_T^t.

At sufficiently low temperature, usually $\leq$4 K, from such a plot the three separate decay rate constants of the spin levels of T_0^t can be obtained. Similarly to the analysis of FF curves for isolated molecules, the steady-state populations of the three T_0^t spin levels can be derived from the amplitudes of the three exponential decays, constituting the total FF curve.

In conclusion, the full sublevel kinetics of the lowest triplet state of a trap, embedded in a collection of isolated pigment molecules transferring singlet-excitation energy to the trap, can be determined using FF curves.

C. FDMR VS. FF

By inserting the kinetic data for the T_0^t state of the trap into Equation 4, the sign of the FDMR transitions of this state, detected via the antenna fluorescence, can be predicted. In the presence of singlet to singlet energy transfer from antenna to trap, the sign of all FDMR transitions is predicted to be opposite to those calculated from the values of k_λ and n_λ^0 obtained from the FF kinetics. For T-T and other types of energy transfer, such sign inversion of FDMR spectra is not predicted, as can be easily concluded from a qualitative analysis of the biomolecular energy transfer kinetics in an optical pumping cycle, including energy transfer between T_0^a and T_0^t states. For photosynthetic pigments in nonordered (bio)polymers or organic glasses, often the triplet state kinetics cannot be determined in a reliable manner. Presumably, this is due to the spread in transition frequencies resulting from the distribution of microenvironments of the pigment in such media. Then, the microwave field is not fully saturating for each site and the response of the fluorescence, following a microwave pulse or step, cannot be fitted by three exponentials. In addition, there may be more fundamental reasons, such as increased spin-lattice relaxation between the triplet sublevels in unordered media, preventing a reliable analysis of the microwave-induced fluorescence response. On the other hand, FF curves do not suffer from this phenomenon and yield a set of kinetic data for each of the triplet sublevels, averaged over the site distribution.

V. CONCLUSIONS AND PERSPECTIVES

The model systems which we have discussed are a collection of photosynthetic pigments embedded in a biopolymer and acting as an antenna for optical excitation of a trap. They are representative of well-characterized models of complexes of chlorophylls with protein,

which show efficient excitation energy transfer and charge separation in plants and photosynthetic bacteria.

In these man-made model pigment-polymer systems, a distinction can be made between those molecules with an antenna function on one hand and traps for excitation energy on the other. The antenna and trap contain several chemically different pigments or pigments in different environments.

In photosynthetic systems at room temperature, traps may consist of reaction centers or at low temperature, impurity traps in the antenna. Higher plants have intricate antenna systems consisting of complexes of protein and various forms of chlorophylls: the light-harvesting complex (LHC), and several forms of antannae associated with each of the two reaction centers. Photosynthetic bacteria have similar antennae, organized in a similar way to plants, but simplified by the presence of only one type of reaction center.

The use of ODMR techniques, in particular the inversion of the sign of FDMR transitions, has given useful information on the trapping of excitation energy in pigment-biopolymer model systems. Both ADMR and FDMR can give structural information on the pigment molecule, which acts as the trap in the complex.

Picosecond laser spectroscopy is a useful technique for studying energy transfer between pigments bound to a biopolymer. However, the results to date are not able to tell us very much more than that the Förster description is probably the correct one and that this is dictated by the "static" interaction of pigment and biopolymer.

It will be necessary to investigate even more complicated models containing many pigment molecules in order to test such concepts as the channeling of energy and its localization in certain subpopulations of pigments. The synthesis of such models is difficult, however it may be unnecessary if current attempts to crystallize the isolated chlorophyll-protein complexes from plants and photosynthetic bacteria prove successful. The determination of the structure of these crystalline samples to a sufficient resolution to obtain the atomic coordinates of the antenna and reaction-center pigments will give us model systems containing both the natural pigments and the natural biopolymer, and moreover with a precisely known three-dimensional structure.

Knowledge of the atomic coordinates of the protein biopolymer (the polypeptide backbone, and especially the amino acid side groups) may allow detailed studies of the dynamic role of the biopolymer in electron transfer and possibly in energy transfer, which could be tested by subpicosecond kinetic experiments.

REFERENCES

1. **Breton, J., Martin, J.-L., Migus, A., Antonetti, A., and Orszag, A.,** Femtosecond spectroscopy of excitation energy transfer and initial charge separation in the reaction center of the photosynthetic bacterium *Rhodopseudomonas viridis, Proc. Natl. Acad. Sci. U.S.A.*, 83, 5121, 1986.
2. **Pellegrino, F.,** Ultrafast energy transfer processes in photosynthetic systems probed by picosecond fluorescence spectroscopy, *Opt. Eng.*, 22, 508, 1983.
3. **Schaafsma, T. J.,** ODMR spectroscopy in photosynthesis I, in *Triplet State ODMR Spectroscopy: Techniques and Applications to Biophysical Systems,* Clarke, R. H., Ed., Wiley-Interscience, New York, 1982, chap. 8.
4. **Hoff, A. J. and Gorter de Vries, H.,** Energy transfer at 1.5 K in some photosynthetic bacteria monitored by microwave-induced fluorescence (MIF) spectra, *Isr. J. Chem.*, 21, 277, 1981.
5. **Markwell, J. P., Thornber, J. P., and Boggs, R. T.,** Higher plant chloroplasts: evidence that all the chlorophyll exists as chlorophyll-protein complexes, *Proc. Natl. Acad. Sci. U.S.A.*, 76, 1233, 1979.
6. **Boxer, S. G.,** Model reactions in photosynthesis, *Biochim. Biophys. Acta,* 726, 265, 1983.
7. **Pearlstein, R. M.,** Chlorophyll singlet excitons, in *Photosynthesis: Energy Conversion by Plants and Bacteria,* Vol. 1, Govindjee, Ed., Academic Press, New York, 1982, 293.

8. **Matthews, B. W. and Fenna, R. E.,** Structure of a green bacteriochlorophyll protein, *Acc. Chem. Res.*, 13, 309, 1980.
9. **Kenkre, V. M.,** Theoretical methods of energy transfer in molecular systems, in *Proc. 4th Int. Seminar on Energy Transfer in Condensed Matter,* Pantoflicek, J. and Zachoval, L., Eds., Society of Czechoslovak Mathematicians and Physicists, Prague, 1981, 54.
10. **Mauring, K., Renge, I., Sarv, P., and Avarmaa, R.,** Fluorescence detected triplet kinetic study of the specifically solvated chlorophyll a and protochlorophyll in frozen solutions, *Spectrochim. Acta,* 43A, 507, 1987.
11. **Zuber, H.,** Structure of light-harvesting antenna complexes of photosynthetic bacteria, cyanobacteria and red algae, *Trends Biochem. Sci.*, 11, 414, 1986.
12. **Deisenhofer, J., Michel, H., and Huber, R.,** The structural basis of photosynthetic light reactions in bacteria, *Trends Biochem. Sci.*, 10, 243, 1985.
13. **Rebane, K. K. and Avarmaa, R. A.,** Sharp line vibronic spectra of chlorophyll and its derivatives in solid solutions, *Chem. Phys.*, 68, 191, 1982.
14. **Miller, J. R.,** Controlling charge separation through effects of energy distance and molecular structure on electron transfer rates, *N. J. Chem.*, 11, 83, 1987.
15. **Parson, W. W.,** Photosynthetic bacterial reaction centers: interactions among the bacteriochlorophylls and bacteriopheophytins, *Annu. Rev. Biophys. Bioenerg.*, 11, 57, 1982.
16. **Gulotty, R. J., Mets, L., Alberte, R. S., and Fleming, G. R.,** Picosecond fluorescence study of photosynthetic mutants of *Chlamydomonas reinhardii:* origin of the fluorescence decay kinetics of chloroplasts, *Photochem. Photobiol.*, 41, 487, 1985.
17. **Van Hoek, A., Vos, K., and Visser, A. J. W. G.,** Ultrasensitive time-resolved polarized fluorescence spectroscopy as a tool in biology and medicine, *IEEE J. Quantum Electron.*, QE-23, 1812, 1987.
18. **Tredwell, C. J., Synowiec, J. A., Searle, G. F. W., Porter, G., and Barber, J.,** Picosecond time resolved fluorescence of chlorophyll *in vivo, Photochem. Photobiol.*, 28, 1013, 1978.
19. **Geacintov, N. E., Husiak, T., and Kolubayev, T.,** Excitation annihilation versus excited state absorption and stimulated emission effects in laser studies of fluorescence quenching of chlorophyll *in vitro* and *in vivo, Chem. Phys. Lett.*, 66, 154, 1979.
20. **Kolubayev, T., Geacintov, N. E., Paillotin, G., and Breton, J.,** Domain sizes in chloroplasts and chlorophyll-protein complexes probed by fluorescence yield quenching induced by singlet-triplet exciton annihilation, *Biochim. Biophys. Acta,* 808, 66, 1985.
21. **Van Hoek, A. and Visser, A. J. W. G.,** Artefact and distortion sources in time correlated single photon counting, *Anal. Instrum.*, 14, 359, 1985.
22. **Van Hoek, A. and Visser, A. J. W. G.,** Pulse selection system with electro-optic modulators applied to mode-locked cw lasers and time-resolved single photon counting, *Rev. Sci. Instrum.*, 52, 1199, 1981.
23. **Van Hoek, A., Vervoort, J., and Visser, A. J. W. G.,** A subnanosecond resolving spectrofluorimeter for the analysis of protein fluorescence kinetics, *J. Biochem. Biophys. Meth.*, 7, 243, 1983.
24. **Vos, K., van Hoek, A., and Visser, A. J. W. G.,** Application of a reference deconvolution method to tryptophan fluorescence in proteins. A refined description of rotational dynamics, *Eur. J. Biochem.*, 165, 55, 1987.
25. **Van Hoek, A. and Visser, A. J. W. G.,** Modelocked and synchronously pumped cw lasers and time-resolved single photon counting: a time resolution study, *Proc. Int. Conf. Lasers '87,* Lake Tahoe, NV, Society for Optical and Quantum Electronics, McLean, VA, 1988, 1083.
26. **Hoff, A. J.,** ODMR spectroscopy in photosynthesis II. The reaction center triplet in bacterial photosynthesis, in *Triplet State ODMR Spectroscopy,* Clarke, R. H., Ed., John Wiley & Sons, New York, 1982, 367.
27. **Chan, I. Y., Sandroff, C. F., and Goldenberg, B. L.,** A high temperature ODMR study of the two crystalline phases of benzil, *Chem. Phys. Lett.*, 61, 465, 1979.
28. **Gillies, R., Spendel, W. U., and Ponte Goncalves, A. M.,** Nanosecond-resolved optically detected magnetic resonance: application to the study of triplet-state spin-lattice relaxation in benzil crystals, *Chem. Phys. Lett.*, 66, 121, 1979.
29. **Trifunac, A. D. and Smith, J. P.,** Optically detected time resolved EPR of radical ion pairs in pulse radiolysis of liquids, *Chem. Phys. Lett.*, 73, 94, 1980.
30. **Benthem, L.,** Tetraphenylporphyrin Dimers: An Optical and Magnetic Resonance Study, Thesis Wageningen Agricultural University, Netherlands, 1984.
31. **Clarke, R. H.,** Zero-field ODMR techniques: nonphosphorescence detection, in *Triplet State ODMR Spectroscopy,* Clarke, R. H., Ed., John Wiley & Sons, New York, 1982, 25.
32. **Momo, F., Sotgiu, A., and Zonta, R.,** On the design of a split ring resonator for ESR spectroscopy between 1 and 4 GHz, *J. Phys. E:*, 16, 43, 1983.
33. **Hardy, W. N. and Whitehead, L. A.,** Split-ring resonator for use in magnetic resonance from 200-2000 MHz, *Rev. Sci. Instrum.*, 52, 213, 1981.
34. **Mehring, M. and Freysoldt, F.,** A slotted tube resonator STR for pulsed ESR and ODMR experiments, *J. Phys. E:*, 13, 894, 1980.

35. **Frenois, C.,** Broadband tunable cavities with helical microstrip lines, *J. Phys. E:*, 17, 35, 1984.
36. **Den Blanken, H. J., Meiburg, R. F., and Hoff, A. J.,** Polarised triplet-minus-singlet absorbance difference spectra measured by absorbance-detected resonance. An application to photosynthetic reaction centers, *Chem. Phys. Lett.*, 105, 336, 1984.
37. **Szalay, L., Tombácz, E., Várkonyi, Z., and Faludi-Dániel, Á.,** Detergent effects on an albumin-chlorophyll complex model of photosynthetic protein-pigment complexes, *Acta Phys. Acad. Sci. Hung.*, 53, 225, 1982.
38. **Kusumoto, Y., Senthilathipan, V., and Seely, G. R.,** Association of chlorophyll with amides on platicized polyethylene particles. III. Unusual spectra of chlorophyll a with *N*-methylmyristamide, *Photochem. Photobiol.*, 37, 571, 1983.
39. **Breton, J. and Nabedryk, E.,** Transmembrane orientation of α-helixes and the organization of chlorophylls in photosynthetic pigment-protein complexes, *FEBS Lett.*, 176, 355, 1984.
40. **Fidler, V., Pancoska, P., Porter, G., Vacek, K., and Blaha, K.,** Pheophorbide a covalently linked to polypeptide: a model system for studying pigment-protein interactions, in *Proc. 4th Int. Seminar on Energy Transfer in Condensed Matter,* Pantoflicek, J. and Zachoval, L., Eds., Society of Czechoslovak Mathematicians and Physicists, Prague, 1981, 172.
41. **Hala, J., Pelant, I., Ambroz, M., Pancoska, P., and Vacek, K.,** Site-selection and Shpolskii spectroscopy of model photosynthetic systems, *Photochem. Photobiol.*, 41, 643, 1985.
42. **Hala, J., Searle, G. F. W., Schaafsma, T. J., van Hoek, A., Pancoska, P., Blaha, K., and Vacek, K.,** Picosecond laser spectroscopy and optically detected magnetic resonance on a model photosynthetic system, *Photochem. Photobiol.*, 44, 527, 1986.
43. **Kooyman, R. P. H.,** Complexes and Aggregates of Chlorophylls, Thesis, Wageningen Agricultural University, Netherlands, 1980.
44. **Hoff, A. J. and Gorter de Vries, H.,** Energy transfer at 1.5 K in some photosynthetic bacteria monitored by microwave-induced fluorescence (MIF) spectra, *Isr. J. Chem.*, 21, 277, 1981.
45. **Boxer, S. G., Kuki, A., Wright, K. A., Katz, B. A., and Xuong, N. H.,** Oriented properties of the chlorophylls: electronic absorption spectroscopu of orthorhombic pyrochlorophyllide a-apomyoglobin single crystals, *Proc. Natl. Acad. Sci. U.S.A.*, 79, 1121, 1982.
46. **Kuki, A. and Boxer, S. G.,** Chlorophyllide-substituted hemoglobin tetramers and hybrids: preparation, characterization, and energy transfer, *Biochemistry*, 22, 2923, 1983.
47. **Boxer, S. G. and Wright, K. A.,** Preparation and properties of a chlorophyllide-apomyoglobin complex, *J. Am. Chem. Soc.*, 101, 6791, 1979.
48. **Wright, K. A. and Boxer, S. G.,** Solution properties of synthetic chlorophyllide-and bacteriochlorophyllide-apomyoglobin complexes, *Biochemistry*, 20, 7546, 1981.
49. **Clarke, R. H., Hanlon, E. B., and Boxer, S. G.,** Investigation of the lowest triplet state of the pyrochlorophyllide a apomyoglobin complex by zero-field optically detected magnetic resonance spectroscopy, *Chem. Phys. Lett.*, 89, 41, 1982.
50. **Boxer, S. G. and Bucks, R. R.,** Chlorophyll-amino acid interactions in synthetic models, *Isr. J. Chem.*, 21, 259, 1981.
51. **Moog, R. S., Kuki, A., Fayer, M. D., and Boxer, S. G.,** Excitation transport and trapping in a synthetic chlorophyllide substituted hemoglobin: orientation of the chlorophyll S_1 transition dipole, *Biochemistry*, 23, 1564, 1984.
52. **Boxer, S. G.,** Structure and energetics in reaction centers and semi-synthetic chlorophyll protein complexes, in *Antennas and Reaction Centers of Photosynthetic Bacteria, Structure, Interactions, and Dynamics,* Michel-Beyerle, M. E., Ed., Springer-Verlag, Berlin, 1985, 306.
53. **van der Waals, J. H. and de Groot, M. S.,** Magnetic interactions related to phosphorescence, in *The Triplet State,* Zahlan, A. B., Ed., University Press, Cambridge, 1967, 101.
54. **Krasnovskii, A. A.,** Delayed fluorescence and phosphorescence of plant pigments, *Photochem. Photobiol.*, 36, 733, 1982.
55. **Krasnovski, A. A., Lebedev, N. N., and Litvin, F. F.,** Phosphorescence and delayed fluorescence of chlorophyll and its precursors in solutions, leaves and chloroplasts at 77 K, *Stud. Biophys.*, 65, 81, 1977.
56. **Naus, J.,** Phosphorescence and Delayed Light Emission of Chlorophyll Pigments, Thesis, Charles University, Prague, 1977.
57. **Kleibeuker, J. F., Platenkamp, R. J., and Schaafsma, T. J.,** The triplet state of photosynthetic pigments. I. Pheophytins, *Chem. Phys.*, 27, 51, 1978.
58. **van der Bent, S. J., de Jager, P. A., and Schaafsma, T. J.,** Optical detection and electronic simulation of magnetic resonance in zero magnetic field of dihydroporphin free base, *Rev. Sci. Instrum.*, 47, 117, 1976.
59. **Clarke, R. H. and Hofeldt, R. H.,** Optically detected zero field magnetic resonance studies of photoexcited triplet states of chlorophyll a and b, *J. Chem. Phys.*, 61, 4582, 1974.

60. **van Dorp, W. G., Schaafsma, T. J., Soma, M., and van der Waals, J. H.,** Investigation of the lowest triplet state of free base porphin; microwave induced changes in its fluorescence, *Chem. Phys. Lett.*, 21, 221, 1973.
61. **van Dorp, W. G., Schoemaker, W. H., Soma, M., and van der Waals, J. H.,** The lowest triplet state of free base porphin: determination of its kinetics of populating and depopulating from microwave induced transients in the fluorescence intensity, *Mol. Phys.*, 30, 1701, 1975.
62. **van der Bent, S. J. and Schaafsma, T. J.,** Interaction of light and microwaves with pheophytins, *Chem. Phys. Lett.*, 35, 45, 1975.
63. **Hoff, A. J. and Cornelissen, B.,** Microwave power dependence of triplet state kinetics as measured with fluorescence detected magnetic resonance in zero field. An application to the reaction center bacteriochlorophyll triplet in bacterial photosynthesis, *Mol. Phys.*, 45, 413, 1982.
64. **Beck, J., Kaiser, G. H., von Schütz, I. U., and Wolf, H. C.,** Optically excited triplet states in the bacteria *Rhodopseudomonas sphaeroides* "wild type" detected by magnetic resonance in zero field, *Biochim. Biophys. Acta,* 634, 165, 1981.
65. **Avarmaa, R.,** Fluorescence detection of triplet state kinetics of chlorophyll, *Chem. Phys. Lett.*, 46, 279, 1977.
66. **Avarmaa, R.,** Fluorescence detection study of molecular triplet states in chlorophyll and related compounds, *Mol. Phys.*, 37, 441, 1979.
67. **Provencher, S. W.,** A Fourier method for the analysis of exponential decay curves, *Biophys. J.*, 16, 27, 1976.
68. **Avarmaa, R. and Schaafsma, T. J.,** Site-selected fluorescence detection of magnetic resonance of protochlorophyll and related chlorophylls, *Chem. Phys. Lett.*, 71, 339, 1980.